Recoupled Polarization-Transfer Methods for Solid-State ^{1}H–^{13}C Heteronuclear Correlation in the Limit of Fast MAS

Kay Saalwächter, Robert Graf, and Hans W. Spiess[1]

Max-Planck-Institute for Polymer Research, Postfach 3148, D-55021 Mainz, Germany

An in-depth account of the effects of homonuclear couplings and multiple heteronuclear couplings is given for a recently published technique for ^{1}H–^{13}C dipolar correlation in solids under very fast MAS, where the heteronuclear dipolar coupling is recoupled by means of REDOR π-pulse trains. The method bears similarities to well-known solution-state NMR techniques, which form the framework of a heteronuclear multiple-quantum experiment. The so-called recoupled polarization-transfer (REPT) technique is versatile in that rotor-synchronized ^{1}H–^{13}C shift correlation spectra can be recorded. In addition, weak heteronuclear dipolar coupling constants can be extracted by means of spinning sideband analysis in the indirect dimension of the experiment. These sidebands are generated by rotor encoding of the reconversion Hamiltonian. We present generalized variants of the initially described heteronuclear multiple-quantum correlation (HMQC) experiment, which are better suited for certain applications. Using these techniques, measurements on model compounds with ^{13}C in natural abundance, as well as simulations, confirm the very weak effect of ^{1}H–^{1}H homonuclear couplings on the spectra recorded with spinning frequencies of 25–30 kHz. The effect of remote heteronuclear couplings on the spinning-sideband patterns of CH$_n$ groups is discussed, and ^{13}C spectral editing of rigid organic solids is shown to be practicable with these techniques. © 2001 Academic Press

Key Words: REDOR; TEDOR; distance measurements; dipolar couplings; recoupling methods; spinning sideband patterns.

INTRODUCTION

The development of high-resolution heteronuclear correlation techniques for the determination of connectivities or dipolar proximities in solid-state NMR has attracted much recent attention, on account of an increased interest in solving structural problems in the solid state. Apart from a multitude of applications to heteronuclear pairs of weakly polarized and less abundant (thus often isotopically enriched) spins such as ^{13}C and ^{15}N (*1, 2*), substantial progress has been made toward taking advantage of ^{1}H as the most abundant nucleus in organic compounds (*3–9*). In most of these experiments proposed for ^{1}H–^{13}C correlation, coherent averaging techniques such as multiple-pulse sequences (*3*) or frequency-switched Lee–Gold-

burg (FSLG) irradiation (*5, 6, 10*) are applied in order to achieve high resolution in the ^{1}H dimension. In addition, dipolar correlation techniques allow for the investigation of dynamics of complex molecules in condensed phases (*11*).

Recently, we introduced a novel heteronuclear multiple-quantum (HMQ) MAS experiment (Fig. 1) for ^{1}H–^{13}C correlation in dipolar solids (*8*), where high resolution in the ^{1}H dimension is achieved by virtue of high B_0 fields ($\omega_L^{1H}/2\pi = 700.13$ MHz) and very fast MAS with spinning frequencies up to 35 kHz. The absence of coherent line-narrowing pulse schemes, which are usually associated with a high sensitivity to experimental imperfections, renders the experiment very robust. The requirements for the spectrometer setup are minimal; only the approximate 90° pulse lengths on both channels have to be determined.

Under very fast MAS, all homo- and heteronuclear dipolar couplings are largely averaged out. Even the strong dipole–dipole coupling between protons in organic solids is simplified by reduction to two-spin correlations (*12, 13*). Our experiment is based on the selective *recoupling* of the heteronuclear dipolar interaction by a REDOR (rotational-echo, double-resonance) π-pulse train (*1*) during the excitation and reconversion periods of an HMQ experiment, the framework of which (corresponding to the 90° pulses represented by black bars in Fig. 1) resembles an HMQ correlation (HMQC) experiment known from solution-state NMR (*14*). The isotropic *J*-coupling, which is used for the excitation and reconversion of the heteronuclear coherences in the solution-state case, does not contribute in this solid-state experiment since it is refocused. One of the aims of this paper is to show experimentally and theoretically that very fast MAS helps in breaking up the tightly coupled homonuclear dipolar coupling network among the protons, such that a treatment of the experiment is appropriate in terms of *heteronuclear couplings only,* with the influence of the homonuclear couplings merely being restricted to the residual ^{1}H linewidth in the correlation spectra. The recoupled heteronuclear dipolar coupling Hamiltonians for all individual pairs commute with each other, and as a result, concepts known from solution-state NMR, which rely on the existence of a limited number of well-localized (usually *J*-) couplings, become applicable.

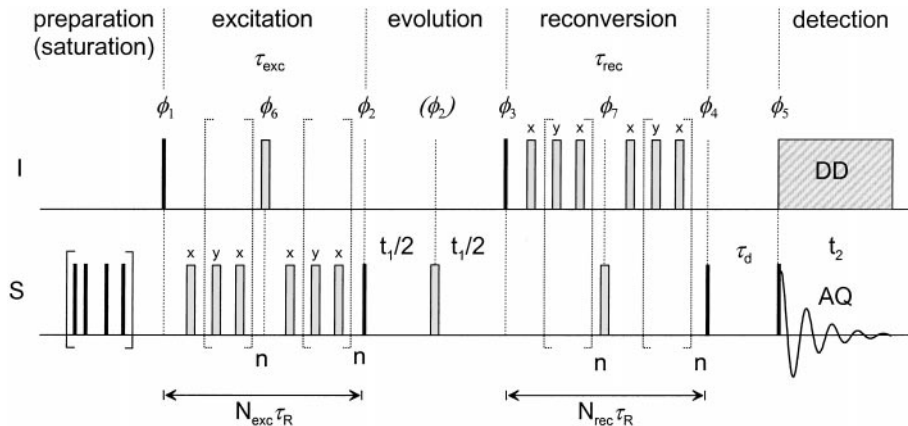---

[1] To whom correspondence should be addressed.

FIG. 1. Pulse sequence for the two-dimensional REPT-HMQC experiment. The relative phases of the π-pulses in the trains are chosen according to the (xy-4) scheme (*38*) and are kept constant during the experiment. All other phases, ϕ_i, are listed in Table 1. Setting $n = 0$ corresponds to a recoupling time of $2\,\tau_R$. For just one rotor period of recoupling, the first π-pulse of each train and the corresponding delays are also omitted. The initial pulses on the S-spin channel represent a saturation pulse train applied in order to suppress signals from initial ¹³C polarization.

The experiment was termed REPT-HMQC, for *re*coupled *p*olarization-*t*ransfer HMQC, in order to account for the fact that initial ¹H magnetization is used directly for the excitation of the heteronuclear coherence states, which are subsequently monitored during the t_1 dimension of a 2D experiment, and then converted to ¹³C magnetization observable in t_2. Apart from the introduction of the t_1 evolution time, the pulse sequence is identical to the previously published TEDOR (trans-ferred-echo, double-resonance) experiment (*15, 16*), which is in principle the one-dimensional version of REPT-HMQC ($t_1 = 0$ in Fig. 1) and is useful for the determination of heteronuclear dipolar couplings between isolated pairs of spins obtained from monitoring the signal intensity as a function of independently chosen excitation and reconversion times. Two-dimensional versions of TEDOR have also been presented (*17–19*), but they all differ from the REPT approach in the way the dipolar coupling information is extracted (vide infra). An alternative approach to the coherent polarization transfer would be to use a CP step to generate initial ¹³C magnetization and to perform the two-dimensional analogue of a REDOR experiment (*20*), where one of the two involved spin species never undergoes evolution as transverse coherence. ¹H–¹³C correlation experiments based on initial ¹³C magnetization exhibit entirely different features compared with REPT when multi-spin systems are considered. These aspects will be dealt with in a separate publication (*21*).

In both TEDOR and REDOR, the formalism originally used for the description of these experiments was not particularly suited to address the possible excitation and measurement of the evolution of heteronuclear multispin coherences such as the mentioned HMQ modes. This aspect has been recognized recently in publications of Jelinski (*20*), Hong and Griffin (*2*), and Schmidt-Rohr (*22*), where ¹³C–¹⁵N and ¹³C–²H HMQ correlation experiments were performed in order to study distances, torsion angles, and site mobility in small peptides,

respectively. A distinct feature of the REPT-HQMC experiment discussed here is the appearance of unusual spinning sidebands in the MQ dimension of the experiment, which can be used to extract quantitative ¹H–¹³C dipolar coupling information. These spinning sidebands appear as a consequence of the explicit t_1 time dependence of the dipolar Hamiltonian during the reconversion period of a 2D MQ experiment (*23, 24*). Characteristically, these spinning sidebands do not map out the anisotropy of the dipolar interaction, but cover a frequency range which is dependent on the product of the strength of the dipolar interaction with the excitation and reconversion times. In homo- and heteronuclear two-spin systems, only odd-order sidebands are expected from theory, while even-order sidebands and a centerband appear as a consequence of either homo- or heteronuclear couplings to additional spins (*25*), chemical-shift anisotropy during t_1 (*7*), or pulse imperfections (*26*). Using L-tyrosine, it was shown (*8*) that strong CH dipolar couplings can be measured very accurately by fitting the relative intensities of such sidebands, which were found to be only weakly perturbed by couplings to additional spins. The emphasis of this paper is to explore the use and practical limits of heteronuclear MQ spinning sideband analysis with respect to weaker couplings and multispin systems.

The paper is structured as follows: in the first section, using product operator formalism (*27*), a brief account of the theoretical treatment of the REPT-HMQC experiment is given, and REPT-HMQ spinning sideband measurements on an isolated CH model system will be presented, which illustrate that very fast MAS successfully removes perturbations from remote protons. Then, in Section 2, it will be shown that the REPT-HMQC technique can be improved for specific applications by changing the coherence state present during t_1. ¹H–¹³C shift correlation spectra obtained with the REPT techniques are compared with other currently used methods, and it is further

shown that spinning sideband patterns can be measured in less time using a specific REPT variant. In Section 3, the theoretical treatment will be extended to multiple couplings of a single ^{13}C to many protons. It is shown that a spinning sideband analysis is feasible even in the multispin case and can be used to determine relatively weak ^{1}H–^{13}C coupling constants. Also, the remaining weak influence of homonuclear ^{1}H–^{1}H couplings on the spectra is investigated more closely. Finally, in Section 4 the straightforward application of one-dimensional REPT techniques for spectral editing applications is illustrated.

1. THE SPIN-PAIR APPROACH UNDER VERY FAST MAS

1.1. Spin-Pair Theory for the REPT-HMQC Experiment

First, we will give a brief account of the description of heteronuclear dipolar couplings under MAS conditions, which forms the basis of the theoretical considerations in this paper. The heteronuclear dipolar coupling of a spin $I^{(i)}$ and one S-spin under MAS is most conveniently treated by using the average Hamiltonian covering the evolution during an interval $(t_a; t_b)$,

$$\bar{H}_{I,S}(t_a; t_b) = \frac{\Phi^{(i)}(t_a; t_b)}{t_b - t_a} 2\hat{I}_z^{(i)}\hat{S}_z, \qquad [1]$$

where $\Phi^{(i)}(t_a; t_b)$ is the dipolar phase factor, which is calculated as the integral over the $m = 0$ spherical-tensor element in the laboratory-frame representation of the second-order dipolar coupling, $A_{20}^{I_iS,\mathrm{LAB}}$:

$$\Phi^{(i)}(t_a; t_b) = \int_{t_a}^{t_b} \frac{1}{\sqrt{6}} A_{20}^{I_iS,\mathrm{LAB}}(\omega_R t)dt, \qquad [2]$$

$A_{20}^{I_iS,\mathrm{LAB}}(\omega_R t)$ is time-dependent by virtue of MAS and depends on the set of Euler angles $\{\alpha_i, \beta_i, \gamma_i\}$, which transform the coupling tensor from its principal-axes system into the rotor frame. Explicit representations are given in the literature (28, 29). For REDOR, i.e., when the sign of the dipolar coupling Hamiltonian is inverted by a π-pulse for every other half rotor cycle, the average phase factor for a full rotor cycle (as indicated by the bar) reads

$$\bar{\Phi}_t^{(i)} = \int_t^{t+\tau_R/2} A_{20}^{I_iS,\mathrm{LAB}}(\omega_R t')dt'$$

$$- \int_{t+\tau_R/2}^{t+\tau_R} A_{20}^{I_iS,\mathrm{LAB}}(\omega_R t')dt' = 2\Phi^{(i)}(t; t+\tau_R/2), \qquad [3]$$

TABLE 1
Phase Cycle for the REPT Pulse Sequences

ϕ_1	$x\bar{x}y\bar{y}\bar{x}x\bar{x}\bar{y}y$ $\bar{x}x\bar{y}yx\bar{x}y\bar{y}$
ϕ_2	$y\bar{y}\bar{x}x\bar{y}yx\bar{x}$
ϕ_3	$yy\bar{x}\bar{x}\bar{y}\bar{y}xx$
ϕ_4	$\bar{x}\bar{x}y\bar{y}xxyy$
ϕ_5	$xxyy\bar{x}\bar{x}\bar{y}\bar{y}$ $\bar{x}\bar{x}\bar{y}\bar{y}xxyy$
ϕ_6	$y\bar{y}\bar{x}x\bar{y}yx\bar{x}$
ϕ_7	$\bar{x}\bar{x}y\bar{y}x\bar{x}y\bar{y}$
ϕ_{rec}	$yy\bar{x}\bar{x}\bar{y}\bar{y}xx$

Note. The phases differ from the ones given in Ref. (8), which gave spectra which were not completely free of artifacts.

where t merely describes a dependence on the initial rotor phase, $\omega_R t$. If only one I-spin is considered, i.e., when the relative orientation of different coupling tensors does not need to be specified, only two of the three Euler angles are of importance, and Eq. [3] reduces to

$$\bar{\Phi}_t = \frac{-D_{IS}}{\omega_R} 2\sqrt{2}\,\sin 2\beta\,\sin(\omega_R t + \gamma). \qquad [4]$$

D_{IS} is the heteronuclear dipolar coupling constant in units of angular frequency, which depends on the internuclear distance, r_{ij}:

$$D_{ij} = \frac{\mu_0 \hbar \gamma_i \gamma_j}{4\pi r_{ij}^3}. \qquad [5]$$

For the following derivation of the t_1 time-domain signal of the REPT-HMQC experiment (Fig. 1), the calculations in this section are limited to a single IS spin pair. Product operator formalism (27) is used for the calculations, with the phases for the individual pulses given in Table 1.

After an initial 90° x-pulse, the resulting $-y$ magnetization evolves under the action of the REDOR-recoupled heteronuclear dipolar coupling:

$$-\hat{I}_y \xrightarrow{N_{\mathrm{exc}}\bar{\Phi}_0 2\hat{I}_z\hat{S}_z} -\hat{I}_y\cos N_{\mathrm{exc}}\bar{\Phi}_0 + 2\hat{I}_x\hat{S}_z\sin N_{\mathrm{exc}}\bar{\Phi}_0. \qquad [6]$$

An HMQ coherence is then created by application of a 90° y-pulse on the S-spins (the remaining $\hat{I}_y$ transverse coherence does not evolve into detectable S-spin magnetization and is therefore omitted):

$$2\hat{I}_x\hat{S}_z\sin N_{\mathrm{exc}}\bar{\Phi}_0 \xrightarrow{\frac{\pi}{2}\hat{S}_y} 2\hat{I}_x\hat{S}_x\sin N_{\mathrm{exc}}\bar{\Phi}_0. \qquad [7]$$

This coherence is subject to chemical-shift evolution during t_1 in both the I- and the S-spin subspaces. However, neglecting

the influence of S-spin chemical-shift anisotropy for the time being, the S-spin isotropic shift is refocused by the π-pulse in the middle of t_1, and thus the HMQ coherence picks up I-spin chemical-shift phase factors according to

$$2\hat{I}_x\hat{S}_x\sin N_{exc}\bar{\Phi}_0 \xrightarrow{\omega_{CS,I}t_1\hat{I}_z} 2\hat{I}_x\hat{S}_x\sin N_{exc}\bar{\Phi}_0\cos\omega_{CS,I}t_1$$

$$+2\hat{I}_y\hat{S}_x\sin N_{exc}\bar{\Phi}_0\sin\omega_{CS,I}t_1. \qquad [8]$$

Sign-sensitive detection in t_1 is implemented by varying the phase of the third 90° pulse (ϕ_3 on I), thus flipping the I-spin part of the HMQ coherence with either the $\cos\omega_{CS,I}t_1$ or the $\sin\omega_{CS,I}t_1$ prefactor to the z-axis. Following the only the cosine component (y-pulse), we obtain

$$2\hat{I}_x\hat{S}_x\sin N_{exc}\bar{\Phi}_0\cos\omega_{CS,I}t_1 \xrightarrow{\frac{\pi}{2}\hat{I}_y}$$

$$-2\hat{I}_z\hat{S}_x\sin N_{exc}\bar{\Phi}_0\cos\omega_{CS,I}t_1. \qquad [9]$$

This antiphase coherence evolves back into observable S-spin magnetization during the reconversion period, where it acquires a $\sin N_{rec}\bar{\Phi}_{t_1}$ phase factor. The two signal components for the indirect dimension of an REPT-HMQC spectrum (i.e., $\omega_2 = 0$) are thus (8)

$$S_x(t_1) = \langle\sin N_{exc}\bar{\Phi}_0 \sin N_{rec}\bar{\Phi}_{t_1} \cos\omega_{CS,I}t_1\rangle, \qquad [10]$$

$$S_y(t_1) = \langle\sin N_{exc}\bar{\Phi}_0 \sin N_{rec}\bar{\Phi}_{t_1} \sin\omega_{CS,I}t_1\rangle, \qquad [11]$$

where the possibility of choosing different recoupling times for the excitation and reconversion periods ($N_{exc} \neq N_{rec}$) has been included. Note that, during the recoupling periods, the S-spin chemical-shift anisotropy (CSA) is *completely* refocused and thus does not contribute to the signal to a first approximation. Only a weak contribution of CSA to the evolution during t_1 remains and will be discussed below.

The above equations form the basis of a two-dimensional experiment, which can be performed in three ways (8): (i) Incrementing t_1 in steps of full rotor cycles ("rotor-synchronized" experiment) leaves only the modulation of the t_1 signal with respect to the isotropic chemical shift $\omega_{CS,I}$ of the I spins (since $\bar{\Phi}_{t_1}$ is periodic with respect to one rotor period), such that a HETCOR spectrum is recorded, in which the intensity of the cross peaks is determined by the heteronuclear dipolar coupling and the number of recoupling cycles $N_{exc/rec}$. After Fourier transformation over t_2, the slice $S(t_1 = 0; \omega_2)$ represents an HMQ-filtered S-spin spectrum (or a TEDOR spectrum). (ii) Incrementing t_1 in smaller steps gives a full HMQ spinning sideband pattern in the ω_1 dimension, as discussed in

Ref. (8), from which the dipolar coupling constant can be derived. (iii) Fixing $t_1 = 0$ and incrementing $N_{exc/rec}$ allows one to study the buildup of HMQ intensity (this is just the TEDOR approach), which represents an alternative way to extract very weak dipolar couplings. However, if sufficient experimental time is available to record full 2D HETCOR spectra, the HMQ buildup can also be studied with I-spin chemical-shift resolution, in which way the contributions of couplings of different I-spins to one S-spin can be unraveled.

1.2. Experimental Test of the Spin-Pair Approach

In Ref. (8) it was shown that REPT-HMQ spinning sideband patterns can be analyzed in terms of isolated spin pairs even in real systems, where the protons form a tightly dipolar-coupled network. In order to experimentally justify this approach more fully, ammonium formate was chosen as a model system for a relatively isolated ¹H–¹³C pair, with the added benefit of a possible "tuning" of remote proton influences by deuteration of the NH_4^+ groups, which is easily achieved by dissolving the sample in D_2O. The preparation and characterization of the sample is described in detail in Ref. (7).

In Fig. 2, spinning sideband spectra of the directly bound CH-pair in ammonium formate measured for different spinning frequencies and recoupling times using the nondeuterated and deuterated formates are compared. At 10 kHz MAS, a relatively clean sideband pattern is obtained for the deuterated compound. As is apparent from the corresponding simulation, the baseline distortions can be explained by the influence of the chemical shift anisotropy, which arises as a consequence of the incomplete refocusing of the CSA during the non-rotor-synchronized t_1 evolution period with the π-pulse in the middle. The term describing this perturbation reads

$$[\cos\Phi_{CS,S}(0; t_1/2) \cos\Phi_{CS,S}(t_1/2; t_1)$$

$$+ \sin\Phi_{CS,S}(0; t_1/2) \sin\Phi_{CS,S}(t_1/2; t_1)], \qquad [12]$$

which can be appended to Eqs. [10] and [11] as an additional factor. $\Phi_{CS,S}(t; t')$ is defined in analogy to Eq. [2] as the average phase acquired under MAS evolution of a spin exhibiting CSA. Explicit representations of Φ_{CS} are given in Refs. ($7, 30$). At faster spinning, this contribution becomes negligible.

In contrast, the 10-kHz MAS pattern for the protonated sample has a considerably lower S/N and broader peaks and exhibits appreciable even-order sideband and centerband intensity. In pure NH_4HCO_2, the closest remote proton is 2.8 Å from the proton of interest, which gives a dipolar proton–proton interaction more than five times smaller than the C–H interaction, not even considering the motional averaging due to rapid tumbling of the NH_4^+ ions. Nevertheless, the large number of perturbing homonuclear couplings from the numerous surrounding ammonium protons, along with an insufficient
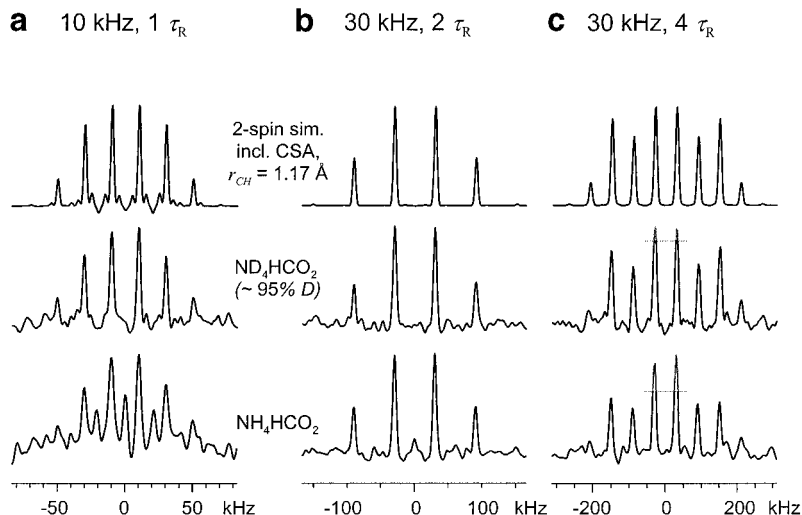
FIG. 2. REPT-HMQ sideband spectra of ammonium formate, measured as bought, i.e., fully protonated (lower traces), and deuterated in the ammonium groups (middle), along with simulated spectra, where the best-fit CH distance and the influence of the chemical shift anisotropy were taken into account. Spinning frequencies and recoupling times were 10 kHz, 1 τ_R (a), 30 kHz, 2 τ_R (b), and 30 kHz, 4 τ_R (c).

suppression of the homonuclear perturbation by MAS, renders the method unsuitable at such "low" spinning frequencies.

The situation changes markedly for a spinning rate of 30 kHz, where the sideband patterns for both compounds are almost the same, except for some residual even-order sideband and centerband contributions for the NH_4HCO_2. Upon increasing the recoupling time, patterns with a large number of sidebands can be generated, allowing for a more accurate determination of the dipolar coupling constant which dominates the pattern. This is the major advantage of the REPT method compared with related separated local-field (SLF) methods (*31, 32*), where under MAS the sideband patterns observed in the dipolar frequency dimension cover only a range which is approximately equal to the coupling constant to be measured. In particular for very fast MAS, conventional SLF sideband spectra would not exhibit higher than first-order spinning sidebands, thus hampering an exact determination of dipolar coupling constants.

At these longer recoupling times (4 τ_R in our case), however, deviations from the ideal behavior are observed in the first-order sidebands, which are higher than expected. This can straightforwardly be explained in terms of contributions from recoupled intermolecular interactions, and these are consequently larger for the protonated compound. However, when the first-order sidebands are excluded from the fit, reliable results can be obtained for both substances. Thus, these experimental results represent encouraging support for the validity of the spin-pair approach. A quantitative treatment of remote spin effects, with the proper distinction of homo- and heteronuclear influences, will be given in the following sections. Moreover, variants of the REPT-HMQC experiment will be proposed, with which the central π-pulse in t_1 can be avoided

and with which spinning-sideband spectra can be acquired in much shorter times.

2. GENERALIZED REPT TECHNIQUES

2.1. Coherence Type Selection during t_1

Even though the REPT-HMQC experiment represents the most versatile approach toward implementing the different ways to perform REPT experiments (HETCOR, sideband spectra, buildup), it exhibits some drawbacks. Apart from the mentioned slight distortions of the spinning sideband patterns due to incomplete refocusing of the CSA interaction, a further disadvantage arises from the inclusion of the π-pulse in the middle of t_1: its finite length leads to synchronization problems, because, for $t_1 = 0$, the pulses with phases ϕ_2 and ϕ_3 (see Fig. 1) should ideally be applied simultaneously on top of a rotor echo. Thus, introducing the π-pulse leads to a timing problem with respect to the t_1 dimension and hence to phase errors in the spectra and signal loss.

Improvements to the technique are straightforward and can be rationalized by following the spin dynamics under the pulse sequence more closely. The possible changes in the sequence involve the timing of the second and third 90° pulse of the REPT-HMQC sequence (ϕ_2 and ϕ_3 in Fig. 1). The joint effect of this pulse pair, i.e., the polarization transfer as the central idea of TEDOR and REPT, is a very famous concept in solution-state NMR, where, owing to the use of *J*-couplings, transfer efficiencies of 100% are theoretically possible. It was published by Morris and Freeman (*33*) under the acronym INEPT (*i*nsensitive *n*uclei *e*nhanced by *p*olarization *t*ransfer) and is one of the most abundant building blocks found in modern solution-state NMR pulse sequences. The theoretical

treatment in the preceding section shows that this transfer can be envisaged to occur via an HMQ coherence, as created by a 90° y-pulse on the S-spins (→ $2\hat{I}_x\hat{S}_x$, Eq. [7]).

An alternative is, however, to apply an I-spin 90° y-pulse first. In analogy to Eq. [7], we write

$$2\hat{I}_x\hat{S}_z\sin N_{exc}\bar{\Phi}_0 \xrightarrow{\frac{\pi}{2}\hat{I}_y} -2\hat{I}_z\hat{S}_z\sin N_{exc}\bar{\Phi}_0. \quad [13]$$

Subsequent application of an S-spin 90° pulse converts the resulting coherence into S-spin antiphase coherence,

$$-2\hat{I}_z\hat{S}_z\sin N_{exc}\bar{\Phi}_0 \xrightarrow{\frac{\pi}{2}\hat{S}_y} -2\hat{I}_z\hat{S}_x\sin N_{exc}\bar{\Phi}_0, \quad [14]$$

which evolves back into observable magnetization during the reconversion period, where it acquires a $\sin N_{rec}\bar{\Phi}_{t_1}$ phase factor.

In this way, the polarization transfer occurs via a two-spin dipolar ordered state (Eq. [13], right-hand side). Moreover, these considerations show that, by manipulation of a two-spin coherence by 90° pulses on either channel, four different types of coherences are accessible in a REPT experiment: two different antiphase coherences (Eqs. [6] and [14]), the HMQ coherence, and the mentioned dipolar-ordered state. For the design of a 2D experiment, the experimentalist is free to chose which of these coherences are to be probed during t_1. In all cases, the reconversion process, in particular the encoding of the reconversion Hamiltonian by the time-shifted rotor phase, $\bar{\Phi}_{t_1}$, occurs in the same way, which means that spinning sideband patterns are generated, no matter which coherence is present during t_1. This demonstrates that reconversion rotor encoding is not specifically a multiple-quantum mechanism, but rather reflects the rotor encoding of the interaction Hamiltonian. In a recent paper, we have shown that in a slightly modified experiment (involving an initial CP), longitudinal magnetization (e.g., as created from the cosine term in Eq. [6]) can also be rotor-encoded to yield sideband patterns which are dominated by even-order sidebands (34).

Pulse sequences designed to probe three of the four mentioned types of coherences during t_1 are depicted in Fig. 3. They differ only in the placement of the t_1 period, and all pulse phases are the same as for the REPT-HMQC experiment. The experiment on top is the familiar REPT-HMQC (see Fig. 1), where the evolution of an HMQ coherence during t_1 necessitates the application of a refocusing π-pulse in the middle of t_1, the disadvantages of which have already been mentioned.

If the proton antiphase coherence given in Eq. [6] is the spin state present during t_1 (second pulse sequence in Fig. 3), there
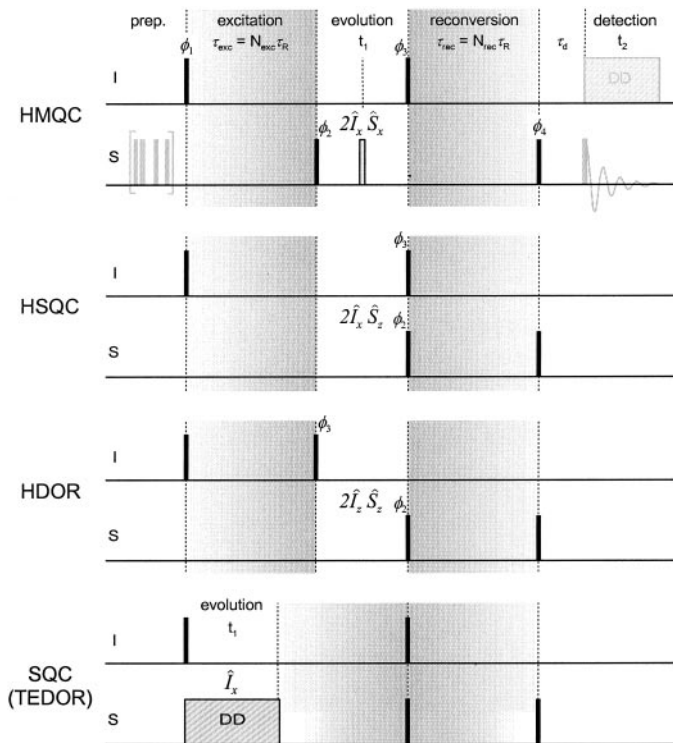

FIG. 3. Variants of the REPT-HMQC experiment. The pulse sequences differ in the placement of the conversion and reconversion pulses (ϕ_2 (=ϕ_4 ± 90°) and ϕ_3 (=ϕ_1 ± 90°) in Fig. 1) with respect to the t_1 period. The recoupling π-pulse trains (in the gray shaded areas) are omitted for clarity, and the pulse phases given in Table 1 are the same for all experiments.

is no need for refocusing any S-spin chemical-shift interaction, since its free time evolution (without recoupling) is governed solely by the I-spin chemical shift. The indirect probing of the time evolution of such an antiphase magnetization has been introduced by Bodenhausen and Ruben (35) for solution-state ¹H–¹⁵N spectroscopy and is referred to as heteronuclear *single-quantum correlation* (HSQC). After t_1, the polarization transfer $2\hat{I}_x\hat{S}_z \rightarrow -2\hat{I}_z\hat{S}_x$ is performed by applying the I- and S-spin 90° pulses simultaneously. In the approximation of neglecting the dipolar evolution of the antiphase coherence (in contrast to the HMQ coherence, the antiphase coherence does evolve under the unrecoupled IS dipolar coupling during t_1), the time-domain signal for REPT-HSQC is identical to that of the REPT-HMQC experiment, given by Eqs. [10] and [11].

The third pulse sequence in Fig. 3 involves the presence of the two-spin dipolar-ordered state (Eq. [13]) during t_1. This state is also termed *longitudinal dipolar order* and has its homonuclear equivalent in the $\hat{T}_{20}$ operator, which, in a $I = 1$ system is also referred to as a spin-alignment state (36). Its important property is that (neglecting homonuclear spin flip–flops with additional spins) it does not undergo time-evolution and is only subject to T_1 relaxation of the involved nuclei. The introduction of a t_1 interval, however, still leads to reconversion rotor encoding, such that a symmetric sideband pattern,
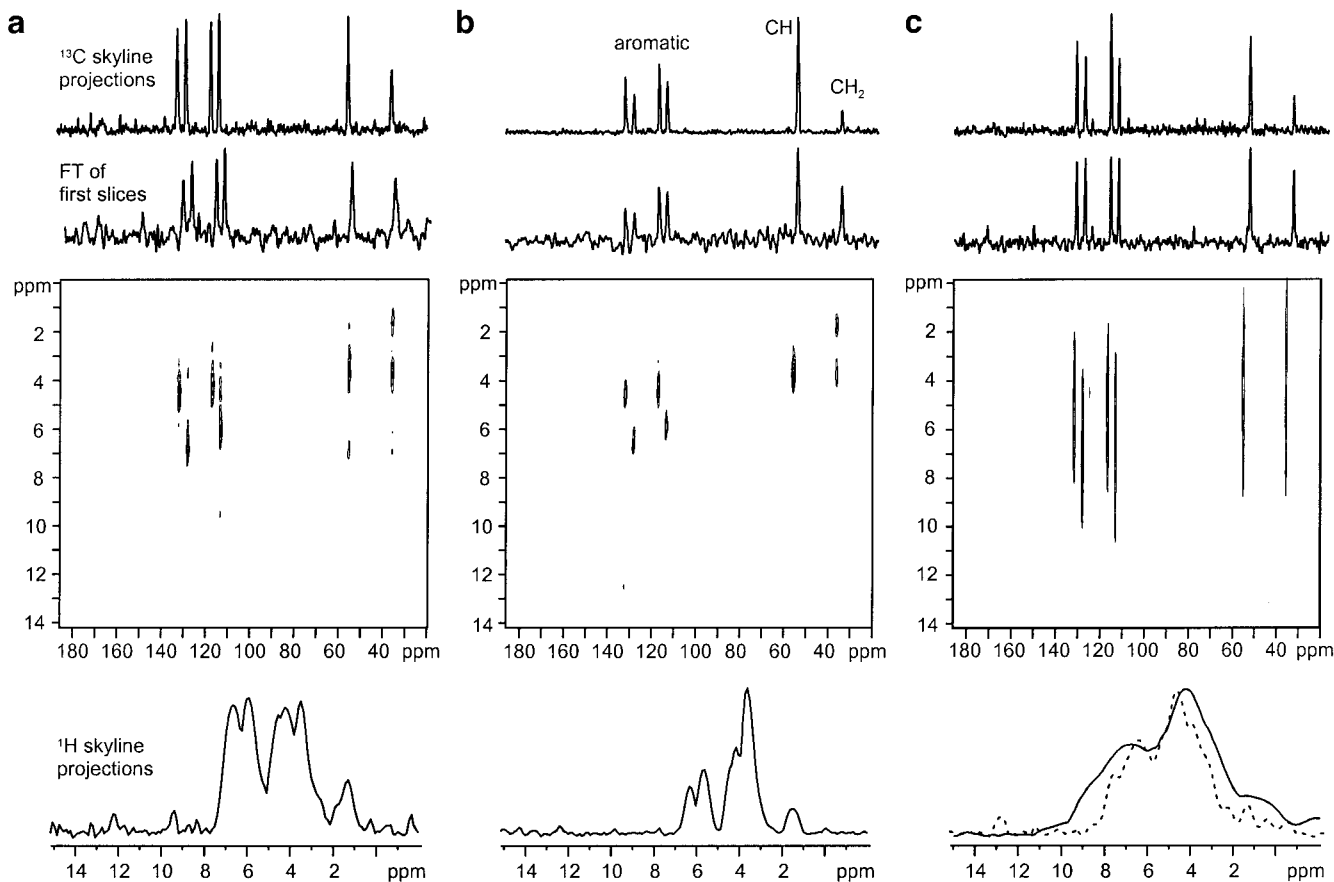
FIG. 4. Comparison of three HETCOR spectra of naturally abundant L-tyrosine · HCl, recorded with 128 transients per slice in each case. (a) An FSLG-decoupled CP correlation spectrum (160-μs contact time with a ramp on ^{1}H varying $\pm 10\%$); and (b) shows an MAS-J-HMQC spectrum (HMQ excitation delay: 1.5 ms). These spectra were obtained with an FSLG decoupling field of 100 kHz, with 192 slices in t_1, amounting to total experiment times of about 7 h. The mean offset and the exact power level for FSLG were optimized on the J-multiplets of the CH and CH$_3$ signals in FSLG-decoupled CP MAS spectra of L-alanine. The REPT-HSQC spectrum shown in (c) was measured at 30 kHz MAS, with a recoupling time of 1 τ_R = 33.3 μs, with 48 slices in t_1 amounting to an experiment time of about 2 h.

centered around zero frequency, is obtained, the time-domain signal of which follows Eq. [10] without the cos $\omega_{CS,I} t_1$ term. This approach helps in saving considerable experiment time and will be discussed below. It will be referred to as *h*eteronuclear *d*ipolar *o*rder *r*otor encoding (HDOR).

The ^{1}H chemical-shift information can also be probed by inserting a t_1 dimension at the beginning of the pulse sequence (bottom experiment in Fig. 3). The polarization transfer then follows as a TEDOR building block consisting of excitation, INEPT transfer, and reconversion. Consequently, rotor encoding does not occur, and the experiment is suitable for recording shift correlation spectra only. This two-dimensional TEDOR experiment (*17, 19*) gives essentially the same result as a rotor-synchronized REPT-HSQC experiment, but since the emphasis of this work is on spinning sideband analysis, this scheme will not be discussed further. Interestingly, one of the earliest HETCOR experiments based on TEDOR (*18*) did have the t_1 dimension placed right before the INEPT transfer, but, since the authors could not yet identify the possible use of t_1

rotor encoding, was later dismissed as experimentally less convenient (*19*). The one-dimensional versions (i.e., $t_1 = 0$) of all of the above-mentioned pulse sequences are identical and correspond to the TEDOR experiment. We will henceforth refer to these as REPT-HMQ-filtered experiments, since this terminology gives the best account of the fact that they can be used to study the buildup and reconversion of *heteronuclear multiple-quantum modes*.

2.2. REPT-HSQC and Comparison of ^{1}H–^{13}C Shift Correlation Methods

Both the REPT-HMQC and REPT-HSQC experiments are suitable for recording high-resolution HETCOR spectra. In this section, we compare a REPT-HSQC correlation spectrum of naturally abundant L-tyrosine · HCl (Fig. 4c), obtained at 30 kHz MAS and a recoupling time of 1 τ_R, with HETCOR spectra of the same sample acquired with two state-of-the-art techniques using FSLG homodecoupling during the ^{1}H chem-

ical-shift dimension. Figure 4 shows a dipolar-based CP correlation spectrum (a), acquired with a very short contact time, so as to restrict the polarization transfer to single-bond distances only (5), and an MAS-J-HMQC spectrum (b), which uses through-bond J-couplings during the FSLG-decoupled HMQ excitation and reconversion intervals (6).

Unfortunately, our 700-MHz spectrometer is not capable of performing the fast phase switching necessary for the FSLG decoupling, so the spectra were acquired on our DSX 500 spectrometer. This loss of ¹H chemical shift resolution is especially damaging in the case of REPT, which achieves its resolution solely from high fields and very fast MAS. All spectra were acquired with 128 scans for each slice, in order to enable a fair comparison of the sensitivity of the different methods. The S/N ratios can be gauged from the Fourier transforms of the first slices and skyline projections over the full 2D spectra shown on top. On the bottom, the skyline projections along the ¹H dimensions allow a comparison of the linewidths in this dimension. In (c), the corresponding projection from a 700-MHz spectrum, as published in (8), is shown as a dotted line. It serves as an example of the possible resolution enhancement achievable by increasing the B_0 field.

Clearly, the two FSLG-decoupled spectra are much superior as far as the ¹H resolution is concerned. The linewidths (full width at half height) are less than 1 ppm, while in the REPT spectrum the lines are more than 3 ppm wide (and decrease to about 2 ppm at 700 MHz). The S/N of all three full 2D spectra, as inferred from the skyline projections, are comparable. However, the REPT spectrum exhibits a superior initial ¹³C signal, as is apparent from the first slices of the 2D spectra. This advantage is clearly more than compensated for by the smaller linewidths of the FSLG-based methods, which leads to an ultimately similar (CP correlation) or better (MAS-J-HMQC) S/N for the full 2D spectra. However, for the REPT spectrum, the maximum resolution in F_1 could be obtained in only 48 slices, while the CP correlation and the MAS-J-HMQC need about four times the number of slices to achieve high ¹H resolution. Especially in the CP case, we did not succeed in measuring a spectrum free of zero-offset artifacts in F_1, which made off-resonance irradiation, and thus a larger spectral width in F_1, necessary. REPT spectra can be acquired with very small spectral widths corresponding to a t_1-increment of 1 τ_R (or even multiples thereof), with on-resonance irradiation on ¹H and TPPI for sign-sensitive detection in F_1. Another clear disadvantage of the REPT approach is the broad and complex CH₂ lineshape, which suffers from the very strong intragroup ¹H homonuclear coupling. As a result, the distinct shifts of the two CH₂ protons, which are different in L-tyrosine·HCl, cannot be resolved.

Although the REPT experiment does not have the best resolution, it has several other advantages: (i) The setup procedure for REPT is simple. Only approximate 90° pulse lengths have to be determined on both channels (see next section for details), while FSLG necessitates an optimization

procedure for the exact values for the frequency switching and the mean offset. Moreover, much effort was involved in first implementing the FSLG techniques on our spectrometer. In particular, finding the right way of simultaneously performing the frequency and phase switch of the FSLG by adjusting the phase presetting time of the pulses so as to remove or reduce artifacts took a considerable amount of time. We found that the FSLG performance sensitively depends on the mean offset, with off-resonance irradiation by about 5 kHz being optimal. This has also been observed by other groups (6). At higher fields, the span of ¹H chemical shifts is large enough such that this condition cannot be fulfilled ideally for all signals involved, which may lead to phase errors such as the ones we observed for the NH_3^+ signal (12.4 ppm) in CP correlation spectra with long contact times. (ii) The chemical-shift information in F_1 is obtained directly in the REPT experiment and can be externally referenced with a simple ¹H SQ MAS spectrum of, e.g., adamantane. A scaling factor characteristic of multiple-pulse homodecoupling, and variations of the mean offset due to frequency switching imperfections, are not of concern. For FSLG, the scaling factor is usually found to be close to the theoretical optimum of $1/\sqrt{3}$, which was used for the axis scaling in Figs. 4a and 4b. However, the mean ¹H offset was not reliable and had to be referenced internally by the known chemical shift of the CH signal. (iii) The increased sensitivity, along with a smaller number of slices in F_1, leads to shorter experiment times for REPT. Sacrificing resolution, the FSLG methods can be acquired with fewer slices, but the overall S/N is then worse.

Finally, some remarks need to be made on possible t_1 artifacts in the case of REPT. Even though, to a first approximation, the time evolution during the t_1 dimension of the REPT-HMQ and REPT-HSQ correlation techniques can be described by the same formula (assuming spin pairs), both experiments differ in their dependence upon contributions from the ¹³C CSA and the residual heteronuclear dipolar interaction. While—within the spin-pair approximation—the REPT-HDOR experiment gives artifact-free sideband spectra, and the 2D TEDOR approach ensures the same for ¹H–¹³C shift correlation spectra, t_1 evolution under chemical-shift anisotropy and heteronuclear dipolar couplings leads to possible artifacts in REPT-HMQC and -HSQC spectra, respectively.

Artifacts arising from CSA evolution of the HMQ coherence were already discussed for the case of REPT-HMQ sideband spectra obtained for ammonium formate (Fig. 2) and are due to the incomplete refocusing of the CSA interaction by the central π-pulse, if $t_1/2 \neq 1 \tau_R$. Therefore, if t_1 is not incremented in steps of 2 τ_R, the correction term given by Eq. [12] also leads to weak artifacts in a shift-correlation spectrum.

For the REPT-HSQC experiment, the antiphase magnetization (and also the in-phase transverse magnetization) is subject to evolution due to residual (unrecoupled) heteronuclear dipolar interaction between the spins constituting the antiphase coherence during t_1:
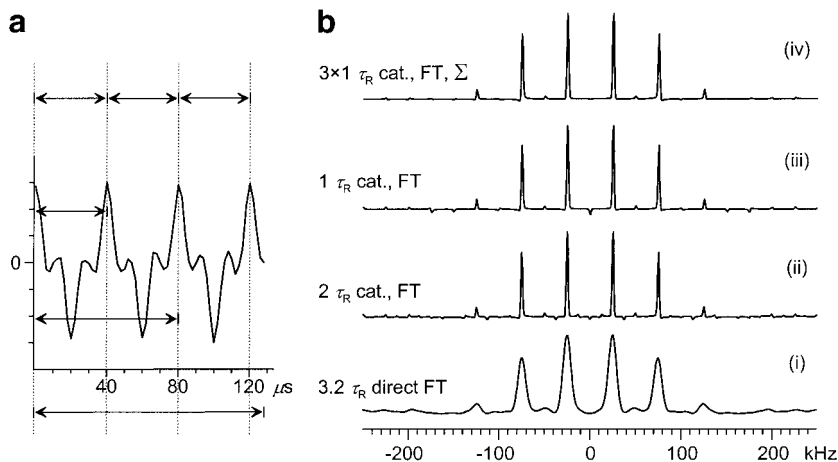
FIG. 5. Processing of the t_1 time-domain signal as obtained from the HDOR experiment. The FID shown in (a), which is measured for the CH$_3$ signal of partially deuterated methylmalonic acid at $\nu_{MAS} = 25$ kHz, with $\tau_{rcpl} = 6\ \tau_R$ and $\Delta t_1 = 2\ \mu$s, consists of 64 points, covering 3.2 rotor periods of encoding with 20 points each. A total of 128 transients were added for each t_1 increment. In (b), Fourier transforms of the indicated parts of the FID are displayed, as discussed in the text.

$$-\hat{I}_y \cos N_{exc}\bar{\Phi}_0 + 2\hat{I}_x\hat{S}_z \sin N_{exc}\bar{\Phi}_0 \xrightarrow{-\Phi(0;\,t_1)2\hat{I}_z\hat{S}_z}$$

$$-2\hat{I}_x\hat{S}_z[\cos N_{exc}\bar{\Phi}_0 \sin \Phi(0;\,t_1)$$
$$-\sin N_{exc}\bar{\Phi}_0 \cos \Phi(0;\,t_1)] + \dots \qquad [15]$$

$\Phi(0;\,t_1)$ is given by Eq. [2]. The final time-domain signal can be obtained from Eqs. [10] and [11] by replacing $\sin N_{exc}\bar{\Phi}_0$ for the above term in square brackets. This correction reduces again to $\sin N_{exc}\bar{\Phi}_0$ in the case of rotor-synchronized shift correlation spectra, since $\Phi(0;\,t_1)$ vanishes for $t_1 = N\ \tau_R$ (which reflects the inhomogeneous nature of the heteronuclear dipolar coupling, in the sense of Maricq and Waugh (*37*)). That is why the TEDOR correlation and the rotor-synchronized REPT-HSQC give largely identical spectra. The influence of the correction term on chemical shift resolved spinning sideband spectra (where $\Delta t_1 \ll 1\ \tau_R$) is also weak, as will be proven in Section 3.

2.3. REPT-HDOR: Spinning Sideband Analysis

Methylmalonic acid, HOOC–CH(CH$_3$)–COOH, was chosen as another useful model compound to study spinning sideband patterns in more detail. It is characterized by a favorable relaxation behavior (allowing for recycle delays of 1 s) and, on account of its CH acidity, is easily obtained in a partially deuterated form following essentially the same procedure given in Ref. (*7*) for ammonium formate. This substance can be used for the study of the influence of remote protons on the spectra of a methyl group, where the closest CH and COOH remote protons can be differentiated from the methyl protons by their chemical shifts. In the partially deuterated form, DOOC–CD(CH$_3$)–COOD, the methyl groups are thus fairly isolated, with the next CH$_3$ proton neighbors being about 4.3 Å

away from the methyl carbon. Using ^{1}H spectroscopy, the degree of deuteration was determined to be about 90% D in the CD and COOD groups.

Figure 5a shows a t_1 time-domain signal of the methyl signal of partially deuterated methylmalonic acid, recorded with the REPT-HDOR sequence. The REPT-HDOR experiment takes advantage of the fact that longitudinal dipolar order does not undergo time evolution during t_1. The amplitude modulation measured as a function of t_1 is thus solely due to the rotor encoding of the reconversion Hamiltonian, which, as is apparent from Eq. [10] with $\omega_{CS,I} = 0$, results in *symmetric* spinning sideband patterns. Since these patterns are centered around the zero offset frequency in the indirect dimension, there is no need for a sign-sensitive detection in t_1, which is needed for all other variants of the REPT technique in order to account for isotropic chemical shift contributions of the protons. The acquisition of a cosine dataset in t_1 thus reduces the experiment time by a factor of 2. The spectral intensity in the sine dataset is zero, thus its presence would only add noise to the final intensity after a two-dimensional Fourier transformation.

Second, as can be inferred from Eq. [10], the signal is *periodic* with respect to the rotor period, and—apart from an increased probability for the occurrence of spin-diffusion effects, which are weak at very fast MAS and will be neglected—the measured modulation pattern decays as a function of the T_1 relaxation times of the nuclei, which are much longer than the rotor period. Experimentally (e.g., Fig. 5a), no appreciable decay of the t_1 signal could be identified in any of the presented measurements. This opens up a number of approaches for the processing of this time-domain signal. Some results of approaches discussed below are presented in Fig. 5b.

The Fourier transform of the whole 3.2 τ_R long FID is shown in slice (i) of Fig. 5b. The applied line broadening (10 kHz) had to be chosen quite large, in order to avoid truncation effects,
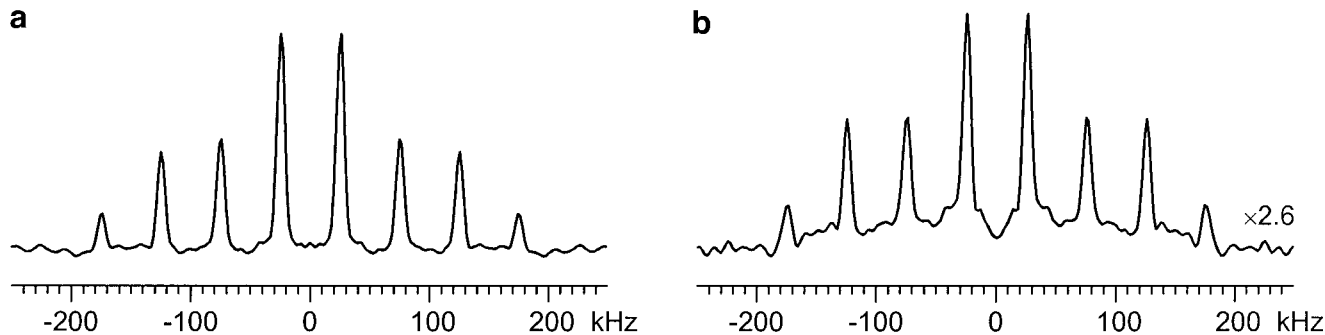
a

b

×2.6

-200   -100   0   100   200 kHz

-200   -100   0   100   200 kHz

FIG. 6. Spinning sideband patterns of the CH_3 group in partially deuterated methylmalonic acid, measured with $\tau_{rcpl} = 10\ \tau_R$ at 25 kHz MAS, (a) under proper setup conditions and (b) using an effective 150° inversion pulse, 20 and 30 kHz offset on the ¹³C and ¹H channels, respectively, and a rotor missynchronization of 100 Hz.

i.e., cutoff sinc wiggles. Narrower sideband linewidths can be obtained by catenating together integer rotor-period blocks of the FID, which allows for an arbitrarily small artificial line narrowing, depending on the number of repetitions chosen. On the timescale of the experiment, no correction is necessary to account for signal decay during t_1.

In principle, it should be sufficient to record just one rotor period of the FID, as can be seen in slice (iii). However, the catenation results in the appearance of *correlated noise,* i.e., random intensity variations of the NMR signal which appear only in the sidebands (up to very high order) of the frequency spectrum, as a consequence of the interplay of the time-translational symmetry of the artificial "FID" and the Fourier transformation. If *two* rotor periods of experimental data are used, noise also appears at *half* rotor period intervals (slice (ii)). Such signals cannot be due to any physical effect, and thus they allow an estimation of the contribution of noise to the sideband intensities. Moreover, noise is seen to be significantly reduced by transforming the sum of the three individually catenated consecutive rotor periods of the time-domain signal (slice (iv)). This approach is useful for the suppression of spectrometer drift effects, when the acquisition time of a single slice is rather long.

2.4. Sensitivity to Experimental Imperfections

It is stated above that the REPT techniques are easy to implement and very robust with respect to the tune-up of the spectrometer; only the approximate 90° pulse lengths have to be determined on both channels. A closer investigation concerning the dependence of absolute spectral (REPT-HMQ-filtered) intensities on several experimental parameters showed that: (i) The sensitivity of the final signal to the effective flip angle of the π-pulse trains is very weak. Deviations of more than 20° from the ideal inversion can be tolerated, with the intensity still at about 80% of the maximum. This broadband nature is mainly due to the (xy-4) phase cycling (*38*). (ii) A dependence of the transferred HMQ intensity on the ¹H and ¹³C offsets is not measurable, on account of the fact that the

majority of the π-pulses in each train is always applied on the channel where only longitudinal terms are involved in the spin dynamics. (iii) Variations of the spinning frequency, which lead to deviations from the ideal $\frac{1}{2}\ \tau_R$ inter-π-pulse spacing, as large as ± 200 Hz (at 30 kHz MAS) can still be tolerated. Using commercial Bruker equipment, the spinning speed is automatically stabilized to ± 10 Hz, such that problems arising from rotor synchronization should be negligible.

In order to give an instructive proof of the robustness of the method, HDOR spinning sideband patterns are compared in Fig. 6 for a proper setup and for deliberately mistuned experimental conditions. Even though the spectral intensity is reduced by a factor of 2.6, the mechanism of sideband generation and its dependence on the mentioned experimental parameters are apparently insignificantly influenced. Sideband analysis is thus demonstrated to be a feasible way to evaluate dipolar couplings even when the experiment is performed in a "quick and dirty" fashion. The distorted baseline in Fig. 6b is due to the severe rotor missynchronization, which made a strong first-order phase correction necessary.

In conclusion, the REPT-HDOR technique is the method of choice for spinning sideband analysis and allows for a substantial decrease in experiment time. The time-domain data in Fig. 5 were obtained in only 3 h (700-MHz spectrometer, ¹³C in natural abundance). If catenation is to be used, only one rotor period of signal would need to be obtained, and the spectrum could be acquired in 1 h. For less well-suited samples (short recycle delay of 1 s, good signal due to well-isolated CH_3-groups), measurement times are mostly less than 12 h.

3. MULTISPIN CONSIDERATIONS

In the last section, spinning sideband patterns due to a methyl group were used to illustrate some general features of patterns generated by the REPT techniques. In order to fully understand all of these features, the theoretical treatment has to be extended to the multispin case. Historically, heteronuclear recoupling methods such as REDOR were established as meth-

ods for the investigation of well-isolated spin pairs. In the solid state, this is usually achieved by using selectively labeled compounds, with considerable isotopic dilution, whereas in the liquid state, the use of *J*-couplings restricts the interactions to the nearest neighbors.

The emphasis of this work, however, is on ^{1}H–^{13}C correlation, where the presence of a tightly coupled proton spin network cannot be neglected. The implications are twofold: Couplings among the protons are strong, and the influence of homonuclear couplings has to be investigated carefully. The results in Section 1 already justified the neglecting of the proton homonuclear coupling at very high spinning speeds, which is largely averaged out by MAS (as opposed to the heteronuclear dipolar interaction, which is recoupled). This has also recently been recognized by Frydman and co-workers (*39*), who were able to perform SLF experiments on rigid crystalline CH systems under moderately fast MAS conditions ($\omega_R/2\pi \leq 14$ kHz) without any further homonuclear decoupling (Historically, ^{1}H–^{13}C SLF spectra were recorded by monitoring the ^{13}C evolution under ^{1}H homodecoupling using multiple-pulse sequences (*31*)). Thus, for sufficiently fast MAS, the short-time behavior of the ^{13}C evolution is simplified by the so-achieved homodecoupling, which allows for an analysis of the data in terms of heteronuclear couplings only. The very fast MAS employed in this publication can even improve on this situation, and at the end of this section results will be presented, which show that the homonuclear influence remains weak even for evolution times exceeding a few rotor periods. These results should contribute to a more complete picture of how the remaining weak homonuclear couplings influence the REPT spectra.

Even more importantly, couplings of the ^{13}C atoms to more than one proton have to be considered. This is of special importance for organic substances, where a theoretical understanding of the spectra of the common structural units, CH, CH$_2$, and CH$_3$, is indispensable. The theoretical treatment of the couplings of an S-spin to multiple I-spins for the REDOR experiment is straightforward and has already been published (*40*). In short, since the heteronuclear dipolar coupling Hamiltonians all commute with each other, $[\hat{H}_D^{SI_i}, \hat{H}_D^{SI_j}] = 0$, the dipolar evolution for individual SI$_i$-pairs can be evaluated *independently,* and product operator theory can be used to calculate the signals. In the following, the analytical calculation of the t_1 time-domain signal for the REPT techniques will be described. Homonuclear couplings will be neglected, which is a well-justified approximation, as will later be proven theoretically and experimentally. Since, due to the noncommutativity of homo- and heteronuclear couplings, $[\hat{H}_D^{SI_i}, \hat{H}_D^{ij}] \neq 0$, a first-order analytical treatment of homonuclear effects is not appropriate. Numerical simulations of the time-evolution of the density matrix will be employed in these cases.

3.1. Heteronuclear Multispin Systems

The REPT technique, with its property of free I-spin evolution during the *excitation* period, is particularly easy to describe: without isotopic enrichment, only *one* coupling partner atom needs to be considered for each proton, i.e., the treatment is restricted to one S-spin and multiple I-spins. This experimental situation is referred to as "proton-detected local field" (*41*) and is characterized by the much simplified coupling topology experienced by a transverse proton coherence evolving in the local field of a single ^{13}C nucleus. The product operator treatment for the excitation period and the INEPT transfer reads

$$-\sum_i \hat{I}_y^{(i)} \xrightarrow{N_{exc}\Sigma_i \bar{\Phi}_0^{(i)}2\hat{S}_z\hat{I}_z^{(i)}}$$

$$-\sum_i (\hat{I}_y^{(i)}\cos N_{exc}\bar{\Phi}_0^{(i)} - 2\hat{I}_x^{(i)}\hat{S}_z\sin N_{exc}\bar{\Phi}_0^{(i)}) \quad [16]$$

$$\xrightarrow{\frac{\pi}{2}\hat{S}_y} \xrightarrow{\frac{\pi}{2}\hat{I}_y} \cdots -\sum_i 2\hat{I}_z^{(i)}\hat{S}_x\sin N_{exc}\bar{\Phi}_0^{(i)}. \quad [17]$$

During reconversion, S-spin antiphase magnetization, $2\hat{I}_z^{(i)}\hat{S}_x$, evolves in the local field of the surrounding protons (SLF situation) and is reconverted to observable S-spin magnetization upon coupling to the *i*th I-spin. Couplings to all the other I-spins add cosine factors to this term, whereas higher antiphase coherences like $4\hat{I}_z^{(i)}\hat{I}_z^{(j)}\hat{S}_y$ (which acquire additional sine phases) are *not* reconverted to observable magnetization.

$$-\sum_i 2\hat{I}_z^{(i)}\hat{S}_x\sin N_{exc}\bar{\Phi}_0^{(i)} \xrightarrow{-N_{rec}\Sigma_i \bar{\Phi}_{t_1}^{(i)}2\hat{S}_z\hat{I}_z^{(i)}}$$

$$\sum_i \hat{S}_y\sin N_{exc}\bar{\Phi}_0^{(i)}\sin N_{rec}\bar{\Phi}_{t_1}^{(i)}\prod_{j\neq i}\cos N_{rec}\bar{\Phi}_{t_1}^{(j)}$$

$$-2\hat{I}_z^{(i)}\hat{S}_x\sin \ldots + 4\hat{I}_z^{(i)}\hat{I}_z^{(j)}\hat{S}_y\sin \ldots \quad [18]$$

The magnetization corresponding to the $\hat{S}_y$ operator is stored along z during the final dephasing delay, and the powder average of its amplitude forms the time-domain signal of the HDOR experiment,

$$S_{REPT}(t_1) = \sum_i \langle \sin N_{exc}\bar{\Phi}_0^{(i)}\sin N_{rec}\bar{\Phi}_{t_1}^{(i)}\prod_{j\neq i}\cos N_{rec}\bar{\Phi}_{t_1}^{(j)}\rangle.$$

$$[19]$$

If chemical-shift evolution of the *i*th I-spin is to be included, *x*- and *y*-components of the signal can be written in analogy to Eqs. [10] and [11] for each of the I-spins. The CSA correction for REPT-HMQC (Eq. [12]) can be appended as an additional

factor, and for the dipolar correction (HSQC), $\sin N_{exc} \bar{\Phi}_0^{(i)}$ has to be replaced by the bracketed expression in Eq. [15].

Moreover, in the case of HMQ evolution during t_1, the HMQ coherence picks up phases due to couplings to additional I-spins, which are not part of the coherence itself. The correction factor is similar to the one given for S-spin t_1 evolution under CSA (Eq. [12]):

$$\prod_{j \neq i} [\cos \Phi^{(j)}(0; t_1/2) \cos \Phi^{(j)}(t_1/2; t_1)$$

$$+ \sin \Phi^{(j)}(0; t_1/2) \sin \Phi^{(j)}(t_1/2; t_1)]. \qquad [20]$$

This correction describes the heteronuclear contribution to evolution rotor modulation (ERM) (25). Its effects will be discussed below. Note that this term is not periodic with respect to t_1-increments of 1 τ_R, such that, in order to prevent artifacts in rotor-synchronized shift correlation spectra (see Fig. 4), t_1 has to be incremented in steps of 2 τ_R, which limits the accessible spectral width.

In the case of *methylene groups,* just one cosine factor appears in Eq. [19]. For the time-domain signal of *methyl groups,* the equation can be simplified to obtain a more descriptive form. In essence, methyl groups undergo fast three-site jumps at ambient temperature, possibly with some distribution of correlation times (42). Therefore, the three heteronuclear couplings have an identical dependence on position, and the average REDOR phases $\bar{\Phi}^{(i)}$, $i = 1 \ldots 3$, for the three protons are equal. The average of a symmetric second-rank tensor, such as the spatial part of the dipolar coupling, undergoing fast symmetric jumps with three or more positions around a specified axis is represented by a uniaxial tensor with its symmetry axis along the rotation axis (30). Therefore, the acquired dipolar phase for a single IS-pair, with S located on the rotation axis, can be calculated using Eq. [3], but with a modified dipolar coupling constant (43),

$$D_{IS}^{app} = D_{IS} \frac{1}{2} (3 \cos^2 \theta - 1), \qquad [21]$$

where θ is the angle between the IS-internuclear vector and the methyl rotation axis. For S-spins located off the rotation axis, the individual $\bar{\Phi}_i^{(i)}$ are still equal, but the averaged dipolar tensor (simply calculated as the average of the three different $\mathbf{A}_2^{D_{IS}}$) will be asymmetric. Consequently, it will explicitly depend on the position of the three individual I-sites relative to the S-spin, yielding a more complicated formula for D_{IS}^{app}. In the off-axis case, Eq. [21] is only a good approximation when $r_{IS} \gg r_{II}$ and when the displacements of the S-spin from the rotation axis are small, i.e., in case of very small asymmetry parameters.

Introducing a single $\bar{\Phi}$ for the three methyl protons, and using the trigonometric relation $\cos^2 a = 1 - \sin^2 a$, we obtain from Eq. [19]

$$S_{REPT}^{CH_3}(t_1) = \langle 3 \sin N_{exc} \bar{\Phi}_0 (\sin N_{rec} \bar{\Phi}_{t_1} - \sin^3 N_{rec} \bar{\Phi}_{t_1}) \rangle$$

$$= \frac{3}{4} \langle \sin N_{exc} \bar{\Phi}_0 \sin N_{rec} \bar{\Phi}_{t_1} \rangle$$

$$+ \frac{3}{4} \langle \sin N_{exc} \bar{\Phi}_0 \sin 3 N_{rec} \bar{\Phi}_{t_1} \rangle, \qquad [22]$$

where for the last line an addition theorem was used. The result has an interesting implication in that it is the sum of two parts, where the first part is the time-domain signal for a single spin pair (with the same apparent coupling constant in the excitation and reconversion periods), and in the second part the apparent coupling constant during reconversion is *three times* the coupling constant during excitation. Since powder averages of the type $\langle \sin Na \sin Nb \rangle$ (note the formal equivalence of this term to a correlation function) approach the value of $\frac{1}{2}$ for $N \to \infty$ and $a = b$ and decay to zero for $a \neq b$, only the first term in Eq. [22] contributes in this limit, and the maximum polarization transfer for a methyl group is $\frac{3}{8} = 37.5\%$.

3.2. Dipolar Couplings from REPT-HDOR and -HSQC Sideband Patterns

Spectra obtained for partially deuterated methylmalonic acid can be used in order to study the applicability of the above formulae, i.e., in the approximation of neglecting homonuclear couplings. Figure 7 shows experimental REPT-HDOR sideband patterns for the CH_3 (a) and the CD (b) carbons recorded with different recoupling times. The latter carbon experiences mainly the rather small heteronuclear couplings from the methyl protons; under the given experimental conditions, weak contributions from residual methyne protons to the sideband patterns of this carbon atom are distributed over many sideband orders and should thus hardly interfere with the analysis of the lower-order sidebands. Both carbon atoms lie on the methyl rotation axis, and Eq. [22] can be expected to hold for the description of the patterns. In all spectra, higher than expected first-order sidebands, which were observed also in the spectra of ammonium formate (Fig. 2), are again apparent. However, using a least-squares fitting procedure based on the Levenberg–Marquardt algorithm, where the higher than first-order sideband integrals were fitted to theoretical intensities obtained by Fourier transformation of the calculated time-domain data (Eq. [19]), yielded dipolar couplings in good agreement with the crystal structure data (Table 2). The available crystal structure of methylmalonic acid (X-ray data, (44)) is somewhat deficient in that the protons are not properly located. For the comparison here, couplings were calculated from an idealized, tetrahedral methyl group (based on a neutron structure of L-alanine (45), with $r_{CH} = 1.09$ Å), with the molecular carbon skeleton from the methylmalonic acid structure. This topic is explained in more detail in Ref. (46).

It was even possible to obtain sideband patterns for the CD carbon, from which dipolar couplings were extracted by fits that also excluded the intensities of the first-order sidebands,
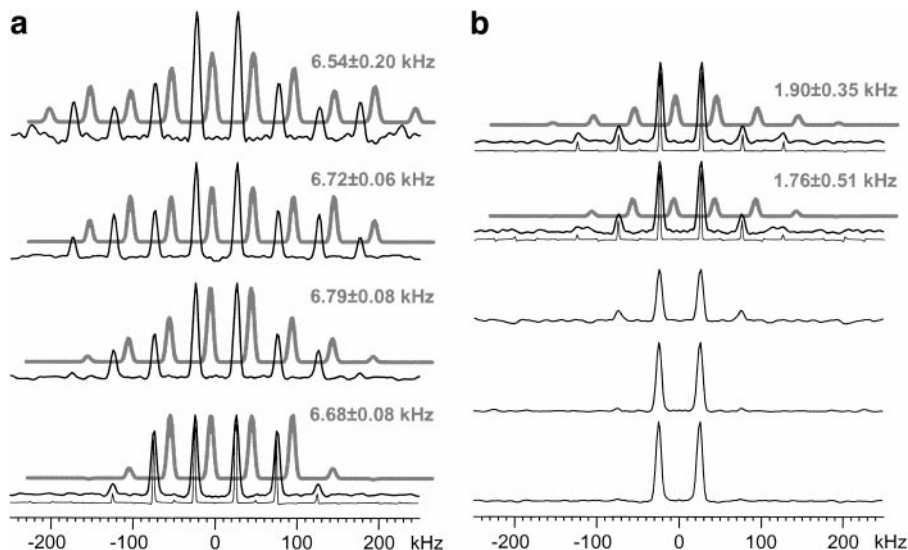
FIG. 7. REPT-HDOR sideband patterns, recorded for a sample of partially deuterated methylmalonic acid at 25 kHz MAS and a total t_1 of 3.2 τ_R. (a) Data for the CH$_3$ carbon, with recoupling times 6, 8, 10, and 12 τ_R, increasing from bottom to top. (b) Data for the CD carbon, with τ_{rcpl} = 6, 8, 18, 24, and 28 τ_R. The gray background traces are the best-fit patterns (with the corresponding results for $|D_{IS}^{app}|$ indicated). The very thin lines are the experimental spectral obtained with the improved processing method; they are the sums of three individual rotor periods of t_1 signal, catenated before Fourier transformation to obtain narrow lines (cf. Fig. 5b, top), while the other spectra were obtained by direct FT of the complete FIDs.

which completely dominate the spectra. Only at very high recoupling times was the fifth-order sideband intensity sufficiently high to allow a reasonable fit. Even though the agreement with the expected values is good, the performance of the method has certainly reached its limit for this measured apparent coupling of 1.8 kHz. Homonuclear effects and perturbations arising from the incomplete isolation of the four involved spins are expected to hamper a sideband analysis beyond this

point. Moreover, the total measured intensity for τ_{rcpl} = 28 τ_R only reached about 20% of the intensity of the spectra with τ_{rcpl} = 6 τ_R, resulting in very long experiment times for a S/N sufficient for a reliable fit of the relatively weak third- and higher-order sidebands.

An important aspect yet to be clarified is the observation of increased first-order sidebands in the measurements for ammonium formate, which were tentatively attributed to contribu-

TABLE 2

Experimentally Observed and Expected Apparent ^{1}H–^{13}C Dipolar Couplings and Bond Lengths for the Methyl Protons in Partially Deuterated Methylmalonic Acid

Sidebands		Fits of NMR data		From crystal structure[a]	
		$|D_{IS}^{app}|/2\pi$ (kHz)	$\Rightarrow r_{IS}$ (Å)	$D_{IS}^{app}/2\pi$ (kHz)[b]	r_{IS} (Å)
CH$_3$		6.68 ± 0.11	1.14 ± 0.01[c]	−7.77	1.09
CD		1.83 ± 0.43	2.22 ± 0.2[d]	−1.97	2.165

Buildup	T_2^{app} (ms)				
CH$_3$	0.93	—	—	−7.77	1.09
CD	0.63	1.33	2.47	−1.97	2.165
CO	0.52	0.78	—	−1.02/−0.96[e]	—

[a] Based on X-ray data (*44*), including an idealized model for the methyl group.

[b] Calculated from the average dipolar tensor of the three proton positions.

[c] Calculated from Eqs. [5] and [21], assuming θ = 109.5°.

[d] Calculated from Eqs. [5] and [21], assuming θ = 28.4°.

[e] Two inequivalent positions in the crystal.

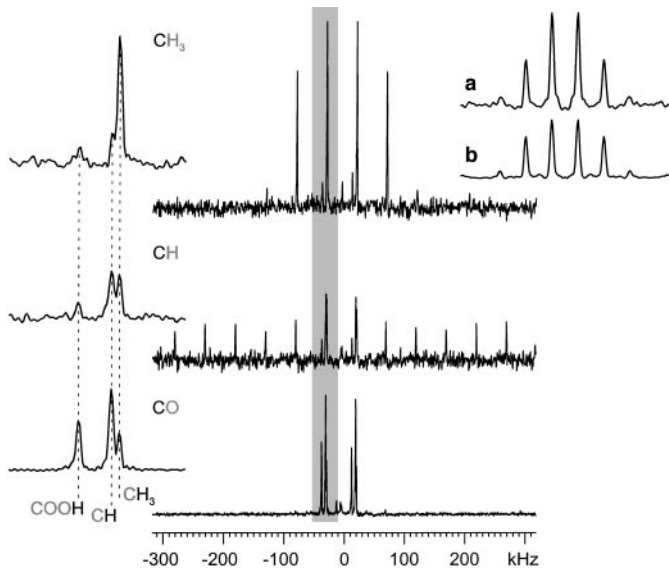**FIG. 8.** REPT-HSQ sideband patterns of methylmalonic acid, recorded at 25 kHz MAS and $\tau_{rcpl} = 6\ \tau_R$. The regions of the first-order sidebands (gray shaded area) have been expanded. Inset (a) is the REPT-HDOR sideband pattern of the CH₃ signal, recorded under the same conditions, which can be compared with the REPT-HDOR pattern of partially deuterated methylmalonic acid, inset (b).

tions of weak remote heteronuclear couplings. An experimental proof of this assumption is presented in Fig. 8. The ¹H chemical shift information, which is present in the t_1 dimension of the REPT-HSQC experiment, can be probed *simultaneously* with the spinning sideband information, if the resolution in this dimension is large enough, i.e., for a sufficient number of acquired slices. The data in Fig. 8 is based on 1024 slices in t_1, with a total acquisition time of about 2 days. Undeuterated methylmalonic acid was used, and the correlations of the respective carbon atoms with the remote protons can, on account of the different chemical shifts, be identified in the first-order sidebands. Consequently, these contributions add up in the REPT-HDOR sideband patterns, where the chemical shift information in t_1 is lost, to give increased first-order sideband intensities, as can be seen in insets (a) and (b). There, REPT-HDOR sidebands of the CH₃ signal are compared for the undeuterated and the partially deuterated form (on which all other measurements in this section were performed). The first-order sidebands measured on the latter sample are still slightly higher than expected; this fact can straightforwardly be attributed to intermolecular remote couplings to other methyl groups.

In the CH₃ HSQC slice, a weak centerband is apparent, which is not present in the CH₃ HDOR patterns in the two insets. Its appearance must therefore be due to effects occurring during the actual t_1 evolution of the antiphase coherence and is indeed explained by the additional dipolar evolution described by Eq. [15]. The effect is seen to be almost negligible

even for a directly bound ¹H–¹³C pair, on account of the averaging achieved by the very fast MAS.

3.3. Dipolar Couplings from 1D REPT-HMQ-Filtered Spectra?

The data obtained from REPT-HMQ-filtered measurements for the same sample are summarized in Fig. 9. As opposed to REDOR data, the REPT (i.e., TEDOR) buildup data cannot be normalized with a reference experiment to yield absolute values for the heteronuclear coherence transfer. As expected, the intensity decreases as a function of the recoupling time after a first maximum is reached. This may tentatively be explained by T_2 relaxation during the recoupling periods. In order to circumvent this relaxation problem, the TEDOR approach relies on keeping the excitation time constant and recording spectra
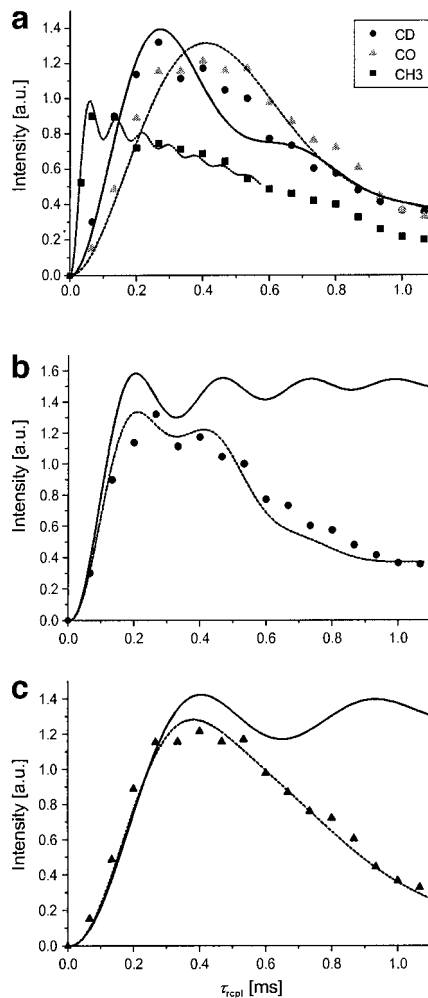

FIG. 9. REPT-HMQ buildup measurements for partially deuterated methylmalonic acid, performed at 30 kHz MAS. (a) Data for all three carbon positions, along with best-fit curves. (b, c) Separately plotted data for the CD and CO carbons, respectively. The curves were calculated from the crystal structure, including only the three protons from the same molecule (solid lines) or 24 further protons from the 8 next-neighbor CH₃ units (dashed lines).

with increasing reconversion time (*16*). The dipolar information is then extracted by analyzing the oscillatory behavior of the intensities. This procedure becomes cumbersome once multiple couplings are involved, which usually lead to a "washing out" of these important oscillations (*47*). By discussing REPT-HMQ-filtered spectra, as obtained by synchronously increasing the N_{exc} and N_{rec}, we do not want to propose an alternative way to determine dipolar coupling constants; rather, we will highlight some of the problems in multispin systems, where a ^{13}C–^{1}H system certainly represents the "worst case."

For the methyl carbon, only the point for $\tau_{rcpl} = 1\ \tau_R$ coincides with the initial rise of the theoretical curve, Fig. 9a, thus hampering an analysis of the buildup behavior. The time resolution of the data for the CD and CO carbon was, however, good enough for a fit to a master curve based on Eq. [22], including an exponential damping function with an apparent transverse relaxation time (T_2^{app}). The results are given in Table 2. Such a fit is only possible if the observed maximum really coincides with the first maximum of the master curve. For cases where relaxation effects are very strong, this cannot be expected, and methods with the option of correcting for such effects have to be chosen. In the present situation, the fits gave reasonable results, which are, however, systematically too low, as a result of the exponential damping. The fit curve for the methyl carbon is based on the average coupling constant from the sideband analyses, and only T_2^{app} has been determined with the fit.

Sideband analysis is thus clearly the method of choice to evaluate the dipolar couplings from REPT experiments. Nevertheless, it is most interesting to note that the data in Fig. 9a can be analytically modeled by using Eq. [19], including the 24 protons of the 8 next-neighbor CH_3 units, with dipolar coupling tensors based on the crystal structure (Figs. 9b/9c). The methyl rotation was accounted for in these calculations by averaging the dipolar tensors from the proton triplets. Even though the scaling of the *y*-axis was adjusted to fit the data, both the position of the maxima and the decay of the signal at longer recoupling times are reproduced in these simulated curves. The observed "apparent" T_2 is thus mainly due to *heteronuclear* couplings to remote protons and can only weakly depend on the "real" T_2 values for ^{13}C and ^{1}H in this system, which are mainly due to homonuclear dipolar dephasing. This notion is supported by the T_2^{app} values in Table 2, which indicate stronger "relaxation" for the carbon atoms which are farther away from the methyl protons. Clearly, the influence of the remote methyl groups increases with an increasing ratio of the remote heteronuclear coupling to the primary intramolecular coupling. These findings represent the most encouraging support for the very weak influence of homonuclear couplings on the spectra, even for longer evolution times.

3.4. Effects of Homonuclear ^{1}H–^{1}H Couplings

So far, the homonuclear couplings among the protons were neglected in the theoretical treatment, and the successful description of most of the spectral features justifies this approximation. Nevertheless, it cannot be expected that an influence of homonuclear couplings is completely absent, and in this section results from measurements and simulations will be presented which give some evidence for weak homonuclear effects.

An analytical treatment of a system evolving under a combined homo- and heteronuclear dipolar coupling Hamiltonian is complex, and instead, numerical density matrix simulations will be used. This approach has the additional advantage that other adverse effects in real experiments, e.g., timing imperfections and finite pulses, can easily be incorporated.

In the first publication of the REPT-HMQC technique (*8*), most π-pulses during excitation were applied on the proton channel, which proved disadvantageous and led to signal loss at longer recoupling times. It is advisable to apply REDOR π-pulses on the channel, where only longitudinal magnetization is to be inverted. In order to explore the nature of this signal loss, HMQ buildup curves, measured for the CD carbon of partially deuterated methylmalonic acid, are compared for the two possibilities in Fig. 10a. The experiment with the pulse train on the protons (the central π-pulse is always applied on the other channel to ensure refocusing of the chemical shift interaction) gives roughly *half* the maximum signal, indicating a strong interplay of the π-pulses and the ^{1}H homonuclear coupling. Four-spin simulations (three methyl protons and the CD carbon) proved that the decrease in maximum intensity is indeed caused by *finite* pulses (open symbols) and not by mere flip-angle deviations. The simulations cannot, however, account for the damping of the intensity at longer recoupling times, which has been shown in the previous section to be due to heteronuclear couplings to numerous remote methyl groups (dotted line). Density matrix simulations with such large numbers of spins are not feasible, and thus it was not attempted to model the data with the many π-pulses on ^{1}H.

In Fig. 10b, the influence of finite π-pulses of varying length, applied to ^{13}C and ^{1}H during excitation, is explored. No difference is discernible when trains with π-pulses of 4- or 8-μs length are applied on the carbon channel, and the simulations confirm this result (again, experimental first-order sidebands are higher than expected). By comparison, the first-order sidebands suffer an intensity loss upon application of the excitation train to the proton channel, and a further slight deterioration is observed for longer pulses, which is also reproduced by the simulations.

Summing up these observations, it is clear that if the experiment is conducted in the most sensible way, that is, avoiding long π pulse trains on the channel where transverse coherences are involved, no significant effects of homonuclear couplings are observable in rigid aromatic systems at spinning frequencies exceeding 20 kHz. One important exception is the CH_2 group, which exhibits the largest ^{1}H–^{1}H coupling found in organic solids. Its value of 23 kHz is of the same order of magnitude as the spinning frequencies applied for the REPT
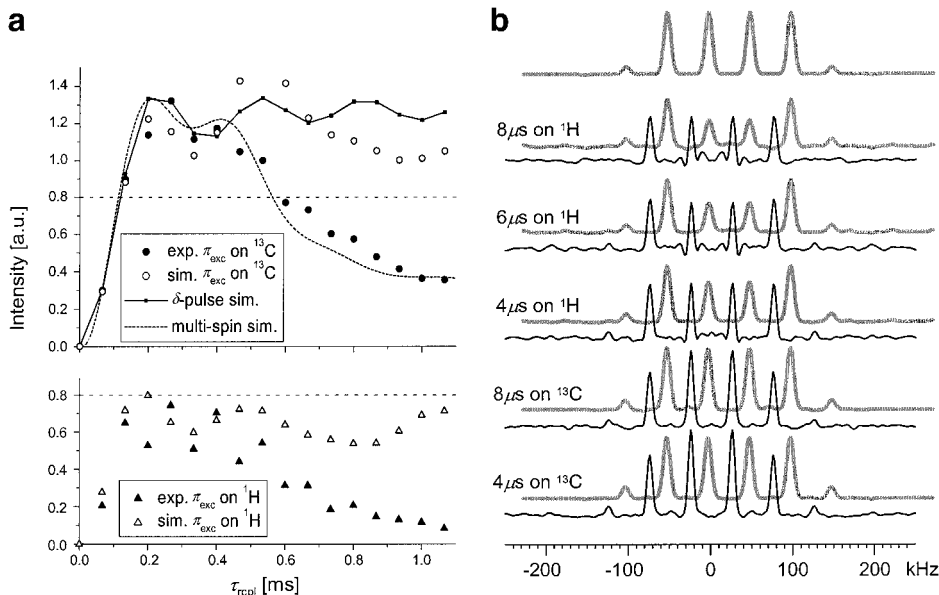
FIG. 10. Buildup data and spectra from experiments on partially deuterated methylmalonic acid ($\omega_R/2\pi = 25$ kHz), showing the influence of homonuclear couplings on the REPT-HMQ intensity buildup for the CH carbon (a), and on REPT-HDOR sideband patterns ($\tau_{rcpl} = 6\tau_R$) of the methyl signal (b). The points in the two diagrams in (a) are plotted on the same vertical scale (with the dashed horizontal lines at $I = 0.8$ for comparison), and the dotted curve in the upper diagram is the same theoretical curve as in Fig. 9b. For the sideband patterns in (b), the π-pulse trains during the excitation period were applied on the carbon and on the proton channel, and the length of the pulses, thus the B_1 field strength, was varied as indicated. The gray background traces are density matrix simulations using the experimental parameters, and for the upper trace, δ-pulses were assumed.

measurements. Unfortunately, it is not possible to study the effect of this strong homonuclear coupling for longer recoupling times, since the methylene signal was shown to vanish for recoupling times longer than just one rotor period (see Fig. 12 below). Patterns obtained for $\tau_{rcpl} = 1\ \tau_R$ do, however, show some characteristic effects.

Spectra for a methylene group, simulated including the homonuclear coupling and calculated from Eq. [19] without homonuclear couplings (gray background traces), are displayed in Fig. 11. As expected, the perturbing heteronuclear coupling to the second proton is strong enough to lead to an almost complete loss of intensity for $\tau_{rcpl} = 2\ \tau_R$, while strong deviations from the spin-pair case are observed for the REPT-HMQC and -HSQC patterns at $\tau_{rcpl} = 1\ \tau_R$. This was proven experimentally for HMQ patterns of the CH$_2$ group in L-tyrosine (8). However, the REPT-HDOR pattern does not exhibit a centerband or unexpected even-order sidebands, indicating that the observed deviations are solely due to effects occuring during t_1.

The simulations for REPT-HSQ and -HMQ sideband patterns in Fig. 11 were calculated using the same artificial line broadening (2.5 kHz) as for the HDOR patterns. Therefore, the observed larger relative line broadenings (thus lower absolute intensities) are due to homonuclear couplings during t_1, while the high centerband intensity for the HSQ spectrum is in part to be attributed to the dipolar correction to the time-evolution formula given by Eq. [15] (note that it is reproduced in the analytical spectrum shown as the background trace). This

effect does not occur when the HMQ coherence is monitored during t_1. Thus, a comparison of REPT-HDOR with REPT-HMQ sideband patterns gives direct evidence for sideband-generating mechanisms active for an HMQ coherence during
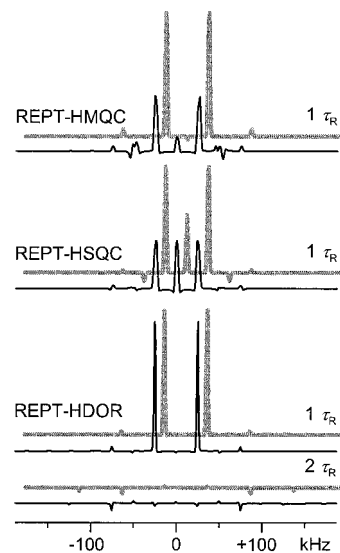

FIG. 11. Sideband patterns from numerical density matrix simulations for a methylene group with $r_{CH} = 1.14$ Å ($D_{CH} = 20.4$ kHz) and an HCH angle of 109.5° at 25 kHz MAS, assuming finite π-pulses of 4-μs length. The recoupling times are as indicated. The gray background traces are analytical results based on Eqs. [15] and [19]. All spectra are plotted on the same vertical scale.
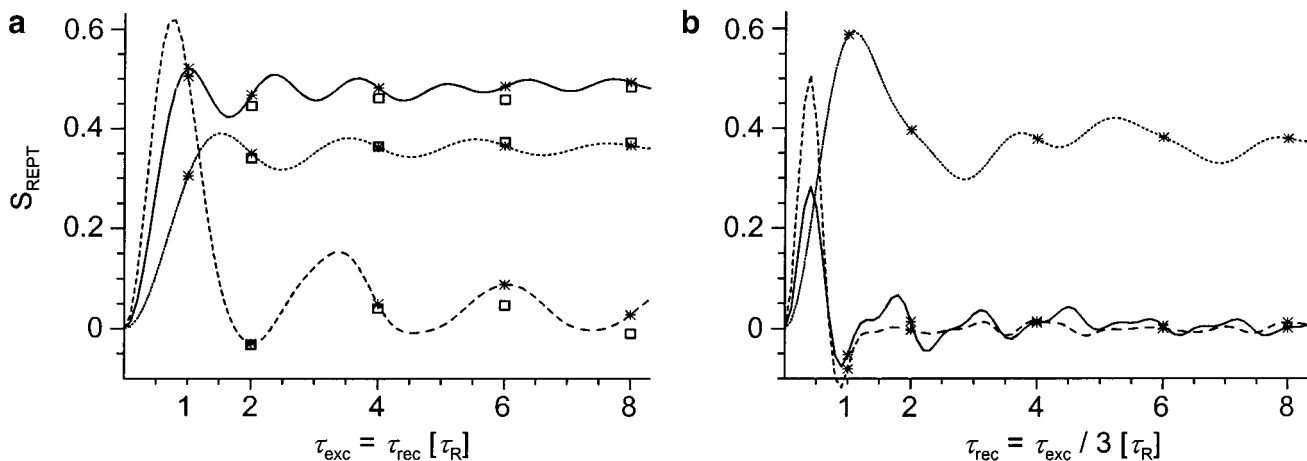
FIG. 12. Buildup master curves for CH (solid), CH_2 (dashed), and CH_3 groups (dotted lines), calculated using Eqs. [19] and [22], under standard conditions, i.e., $\tau_{exc} = \tau_{rec}$ (a), and for $\tau_{exc} = 3\,\tau_{rec}$ (b). The experimentally accessible points for rigid moieties at 25 kHz and reconversion times of 1, 2, 4, 6, and 8 τ_R are indicated by asterisks. The squares in (a) are results from density matrix simulations additionally including homonuclear couplings and finite π-pulses of 4-μs length.

its t_1 evolution (so-called *e*volution *r*otor *m*odulation, ERM (*25*)), to be differentiated from the sideband generation via the explicit time-dependence of the reconversion Hamiltonian relative to the excitation Hamiltonian (*r*econversion *r*otor *e*ncoding, RRE), which is equally active for the HMQ coherence and the dipolar-ordered state. In particular, the influence of homonuclear couplings to additional protons manifests itself more strongly in HMQC sideband patterns.

This result therefore again stresses the advantage of the HDOR approach, where the only possible evolution during t_1 is homonuclear spin flip–flops, the influence of which is apparently negligible. The REPT-HDOR experiment is thus well suited to study the effect of RRE in a well-isolated fashion.

In summary, homonuclear effects cannot be neglected if the π-pulses are applied to the proton channel during excitation, and the interplay of proton transverse magnetization, homonuclear couplings, and finite π-pulses leads to HMQ signal loss and distortions in the spinning sideband patterns. These effects are reminiscent of the results of Goetz and Schaefer (*40*), who observed deviations from the ideal REDOR dephasing in CF_2-groups, where the different chemical shifts of the flourine atoms within these groups, together with the rather strong flourine homonuclear coupling, were identified as the source of error. In a paper of Gullion and Vega (*48*), it was shown that the presence of an isotropic chemical shift difference leads to dephasing in homonuclear experiments where π-pulses are applied once per τ_R. In both cases, the isotropic chemical shift difference is identified as a necessary prerequisite for the observation of distortions due to the homonuclear coupling. The effect observed here is new in that not the isotropic chemical shift but rather finite pulses introduce the homonuclear effects. Further theoretical work is necessary to explore the nature of this effect, especially since the effects of finite

pulses on REDOR recoupling have not yet been investigated in detail.

4. SPECTRAL EDITING APPLICATIONS

The analytical treatment in Section 3.1 suggests the investigation of the buildup behavior of the spectral intensity of CH, CH_2, and CH_3 groups, as measured in 1D HMQ-filtered spectra, as a method to differentiate between these characteristic building blocks. Figure 12a shows results of analytical simulations for these moieties, assuming CH distances of 1.14 Å and perfectly tetrahedral (sp^3-hybridized) carbon atoms. Even at spinning speeds of 25 kHz, the rising part of the curves cannot be probed, as indicated by the asterisks. The methylene curve exhibits the striking feature of rapidly decaying to intensities close to zero for recoupling times larger than 1 τ_R. This has already been described in relation to the L-tyrosine measurements presented in Ref. (*8*) and is here shown to be explicable in terms of the simple theory based on heteronuclear couplings only.

As is obvious from Eq. [22], the rapid three-site jumps of methyl groups result in three identical dipolar coupling tensors and thus lead to contributions to the HMQ-filtered signal proportional to $\frac{3}{4}\langle \sin N_{exc}\bar{\Phi}_0 \sin N_{rec}\bar{\Phi}_0\rangle$ and $\frac{3}{4}\langle \sin N_{exc}\bar{\Phi}_0 \sin 3N_{rec}\bar{\Phi}_0\rangle$, where the former term explains the plateau value for the intensity at 37.5%. The latter term suggests that an experiment conducted with $\tau_{exc} = 3\,\tau_{rec}$ should also lead to the observation of a plateau intensity, whereas the methyne and methylene signals should go to nearly zero at $\tau_{rec} > 1\,\tau_R$. This is shown in Fig. 12b.

These results suggest that only a few 1D experiments, with excitation and reconversion times as discussed, should be sufficient for the differentiation of the four basic structural
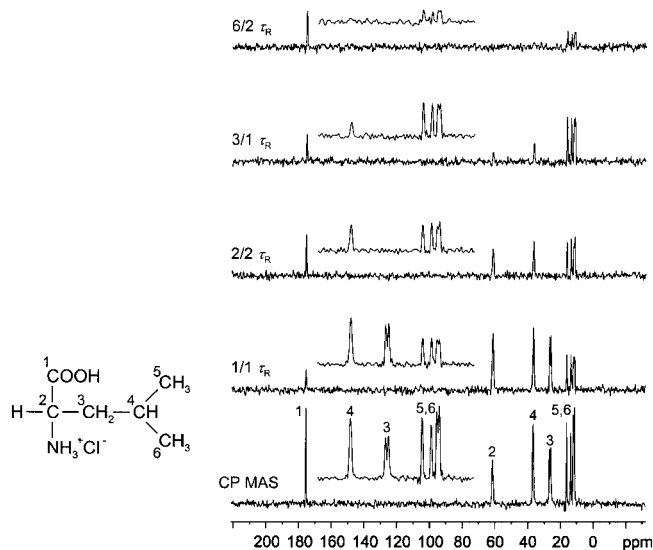
FIG. 13. REPT-HMQ-filtered spectra of L-isoleucine, measured at 25 kHz MAS, with excitation and reconversion times as indicated. The assignments in the CP-MAS spectrum (bottom trace) are according to (*53*). The multiple methylene and methyl lines are due to different crystallographic sites.

units in organic molecules, methyl, methylene, methyne, and quaternary carbons. A test of this spectral editing approach was performed on the amino acid L-isoleucine, which contains all four kinds of carbon atoms; the results are shown in Fig. 13.

Methylene signals are most easily identified. Upon changing τ_{exc} and τ_{rec} from 1 τ_R to 2 τ_R, they vanish completely. The transition to the spectra acquired under the asymmetric condition should, according to Fig. 12b, lead to the disappearance of the CH signals, which is experimentally observed for 6/2 τ_R. The—albeit—weak presence of these signals in the 3/1 τ_R spectrum might be due to contributions of remote spins and indicates deviations from the simple theory. As expected, the methyl intensities decrease with increasing recoupling times in the asymmetric spectra, whereas the quaternary carbon signal increases. Since the signal of quaternary carbons is more sensitive to local dipolar couplings to remote spins, this cannot be taken as a rule, even though experiments on other samples indicated the same behavior.

In summary, methyne and methylene signals can unambiguously be identified with these 1D filtered spectra, whereas some uncertainty remains for the quaternary and methyl signals. Nevertheless, the acquisition of a REPT-HDOR sideband pattern with $\tau_{rcpl} = 6 \, \tau_R$ at 25 kHz MAS is a possible way to achieve an *unambiguous* assignment. Such a spectrum will yield the familiar pattern for a methyl group (see Figs. 5 or 8), and a spectrum dominated by first-order sidebands for quaternary carbons. CH groups in turn show a multitude of spinning sidebands up to 13th order.

Considerable research efforts have been devoted to the development of spectral editing techniques in the solid state. Among the first approaches were separated local field methods

(*49*), CP-based methods (*50–52*) using the concepts of polarization inversion or depolarization, and, finally, methods utilizing ¹H–¹³C *J*-couplings (*53*). Only recently, improved protocols based on the CP methods have been published (*54, 55*), which were necessary in order to obtain cleaner spectra and to remove some ambiguity in differentiating quaternary and methyl carbons. Clearly, the approach based on *J*-coupling is the only one which is not critically influenced by molecular motion. Common to the previous dipolar-based methods are pulse sequences that require very careful setup, while the construction of edited spectra involves critical relative weighting of intensities of spectra measured under different conditions. The concepts presented here are, by comparison, based on a very simple pulse sequence, and CH and CH_2 groups can easily be identified by comparison of four spectra, with some ambiguity only remaining for methyl and quaternary carbons, while a single 2D spectrum (with a minimum of only about 20 slices in t_1) can be used for an unambiguous assignment.

CONCLUSIONS

In this paper, we have shown that ¹H–¹³C correlation via REDOR-type recoupling of the heteronuclear dipolar interaction at very fast MAS is feasible. In particular, the effects of homonuclear couplings were found to be almost negligible on the relatively short recoupling timescale of several rotor periods.

Several implementations of the REPT technique were presented, and different variants are suitable for specific applications. All of these are applicable to only 10 mg of a powdered sample of moderately sized organic molecules with ¹³C in natural abundance. It should be emphasized that, even though for HETCOR applications, high B_0 fields are essential to obtain sufficiently well-resolved spectra, the spinning sideband applications may just as well be performed in lower magnetic fields. Only very fast MAS (20–30 kHz) is necessary for the suppression of perturbing homonuclear couplings.

The **REPT-HSQC** is the method of choice for **heteronuclear ¹H–¹³C shift correlation,** i.e., rotor-synchronized 2D spectra. Spinning sidebands *can* also be obtained using this sequence (as shown in Fig. 8), and these consequently contain chemical-shift information. This information is useful only when contributions of different protons to a spinning sideband pattern of a specific carbon nucleus are to be separated. However, the high resolution in t_1 needed for this application, and thus the large number of slices to be acquired, limits the applicability of this approach.

Spinning sideband patterns are most conveniently measured with the **REPT-HDOR** sequence, as the dipolar coupling information is obtained within the shortest possible experimental time. The loss of chemical-shift information in t_1 means that the ¹H nucleus involved in the coupling constant reflected in the pattern has to be known. This complementary information can be obtained by measuring a shift correlation

spectrum separately, if no reasonable assumption is available. The pattern always reflects the strongest pair coupling in a CH_n system, and the contributions of weak secondary couplings are present only in the first-order sidebands, which can be excluded from the fit. If no coupling is dominant, the measurement of a chemical-shift resolved pattern (using REPT-HSQC) cannot be circumvented.

Finally, on account of the very fast MAS frequencies used in these experiments, homonuclear ^1H–^1H effects were found to be virtually absent in most realistic systems (with the two exceptions of methylene groups and when the excitation π-pulse train is applied to the protons). The modulation of the coherence evolving in t_1 by homonuclear, and, more importantly, by heternuclear couplings to additional ^1H spins was shown to be absent in REPT-HDOR spinning sideband patterns. Only when the effect of **evolution rotor modulation** due to additional protons is to be investigated does the comparison of HDOR with **HMQC** sideband patterns allow the quantification of these effects. REPT-HSQC patterns are slightly distorted by the dipolar t_1 evolution of the spin-pair antiphase coherence itself (Eq. [15]), while the REPT-HMQC suffers complications due to the timing problem introduced by the central π-pulse, which leads to small phase errors in t_1 and a slightly reduced overall intensity.

The REPT techniques hold particular promise for dynamics applications, where the reduction of heteronuclear dipolar couplings due to fast motional averaging can be studied in a quantitative fashion. The REPT-HDOR experiment can in some way be considered a fully quantitive analogue of the familiar WISE (*wi*deline *se*paration) technique for the study of mobility in polymers (*56*), without sacrificing its experimental simplicity. A first application of REPT spinning sideband analysis to determine a dynamic order parameter in discotic liquid-crystalline phases has already been published (*11*). Also, interesting changes in ^1H chemical shifts as a result of π–π packing effects (*57*) could be resolved using REPT-HSQ shift correlation spectra.

REPT-HSQC and REPT-HDOR are routinely used in our lab to obtain ^1H–^{13}C HETCOR spectra and proofs of rigidity or indications of fast dynamics, respectively, where even for more complex systems like dendrimers, polymers, or supramolecular systems, quality spectra are usually obtained within half a day of measuring time with ^{13}C in natural abundance and using less than 15 mg of sample. Generally, compared with the rigid crystalline solids used in this paper, the ^1H lines observed in disordered systems, such as amorphous polymers, are mostly heterogeneously broadened, such that the line narrowing afforded by very fast MAS using the simple REPT approach is often sufficient. Also, if the sample in question is partly mobile and thus less strongly coupled, as is the case for, e.g., liquid-crystalline mesophases, REPT-HSQC spectra will also be sufficiently well-resolved, without recourse to the increased experimental effort involved in setting up FSLG homodecoupled HETCOR experiments.

Preliminary results were obtained for very weak residual dipolar couplings in polymer melts, which are a measure of the local order parameter of individual chain segments on the NMR timescale. To date, homonuclear ^1H double-quantum buildup data have been used to investigate such effects (*58*). Applying the new REPT-HDOR approach, initial results indicate the possibility of obtaining spinning sideband patterns exhibiting enough higher-order sideband intensity to determine residual heteronuclear dipolar couplings of a CH group on the order of 200 Hz, yielding supplemental information on local order. However, little is known about how motions on the NMR timescale, i.e., the intermediate motional regime, affect the mechanism of sideband generation by rotor encoding. Investigations along these lines are underway and are expected to open up the way to obtaining information from systems naturally abundant in ^{13}C, which was up until now only accessible using ^2H NMR.

EXPERIMENTAL

Instrumentation. The NMR experiments were carried out on digital Bruker Avance-type instruments, with B_0 fields corresponding to ^1H resonance frequencies of 300.23 MHz (DSX300, 7-T wide-bore magnet), 500.13 MHz (DSX500, 11.7-T wide-bore magnet), and 700.13 MHz (DRX700, 16.4-T narrow-bore magnet). Most of the data were measured on the DRX700. The spectra measured on ammonium formate (Fig. 2) were the only ones measured on the 300-MHz spectrometer, and the shift correlation spectra in Fig. 4 were obtained at 500 MHz. Commercial 2.5-mm MAS double-resonance probes, also manufactured by Bruker, were used, with 90° pulses of 2-μs length (corresponding to $\omega_1/2\pi = 125$ kHz) on both channels and the same field strength for the dipolar decoupling. In all experiments, TPPM dipolar decoupling (*59*) was employed, using approximate 160° pulses and a phase-modulation angle of 30°.

Samples. Natural abundance ammonium formate, L-tyrosine, and methylmalonic acid were bought from Aldrich. The hydrochloride of L-tyrosine rather than the pure amino acid was used because of the more favorable T_1 relaxation time of the former. It was prepared by dissolving L-tyrosine in dilute HCl and subsequently evaporating the solvent. The procedure was repeated twice. The deuteration procedure for ammonium formate, which was also used for the partially deuterated methylmalonic acid sample, is described in Ref. (*7*). The degree of CH/COOH deuteration of methyl malonic acid sample was determined to be about 12% (mol) using ^1H SQ MAS NMR spectra.

REFERENCES

1. T. Gullion and J. Schaefer, Detection of weak heteronuclear dipolar coupling by rotational-echo double-resonance nuclear magnetic resonance, *Adv. Magn. Reson.* **13**, 57–83 (1989).

2. M. Hong and R. G. Griffin, Resonance assignments for solid peptides by dipolar-mediated ^{13}C/^{15}N correlation solid-state NMR, *J. Am. Chem. Soc.* **120**, 7113–7114 (1998).

3. A. Bielecki, D. P. Burum, D. M. Rice, and F. E. Karasz, Solid-state two-dimensional ^{13}C–^{1}H correlation (HETCOR) NMR spectrum of amorphous poly(2,6-dimethyl-*p*-phenyleneoxide) (PPO), *Macromolecules* **24**, 4820–4822 (1991).

4. W. Sommer, J. Gottwald, D. E. Demco, and H. W. Spiess, Dipolar heteronuclear multiple-quantum NMR spectroscopy in rotating solids. *J. Magn. Reson. A* **113**, 131–134 (1995).

5. B.-J. van Rossum, H. Förster, and H. J. M. de Groot, High-field and high-speed CP-MAS ^{13}C NMR heteronuclear dipolar-correlation spectroscopy of solids with frequency-switched Lee–Goldburg homonuclear decoupling, *J. Magn. Reson.* **124**, 516–519 (1997).

6. A. Lesage, D. Sakellariou, S. Steuernagel, and L. Emsley, Carbon–proton chemical shift correlation in solid state NMR by through-bond multiple-quantum spectroscopy, *J. Am. Chem. Soc.* **120**, 13194–13201 (1998).

7. K. Saalwächter, R. Graf, D. E. Demco, and H. W. Spiess, Heteronuclear double-quantum MAS NMR spectroscopy in dipolar solids, *J. Magn. Reson.* **139**, 287–301 (1999).

8. K. Saalwächter, R. Graf, and H. W. Spiess, Recoupled polarization transfer heteronuclear multiple-quantum correlation in solids under ultra-fast MAS, *J. Magn. Reson.* **140**, 471–476 (1999).

9. B.-J. van Rossum, C. P. de Groot, V. Ladizhansky, S. Vega, and H. J. M. de Groot, A method for measuring heteronuclear (^{1}H–^{13}C) distances in high speed MAS NMR, *J. Am. Chem. Soc.* **122**, 3465–3472 (2000).

10. A. Bielecki, A. C. Kolbert, and M. H. Levitt, Frequency-switched pulse sequences: Homonuclear decoupling and dilute spin NMR in solids, *Chem. Phys. Lett.* **155**, 341–346 (1989).

11. A. Fechtenkötter, K. Saalwächter, M. A. Harbison, K. Müllen, and H. W. Spiess, Highly ordered columnar structures from hexa-*peri*-hexabenzocoronenes—Synthesis, X-ray diffraction, and solid-state heteronuclear multiple-quantum NMR investigations, *Angew. Chem. Int. Ed. Engl.* **38**, 3039–3042 (1999).

12. C. Filip, S. Hafner, I. Schnell, D. E. Demco, and H. W. Spiess, Solid-state nuclear magnetic resonance spectra of dipolar-coupled multi-spin systems under fast magic angle spinning, *J. Chem. Phys.* **110**, 423–440 (1999).

13. I. Schnell and H. W. Spiess, High-resolution ^{1}H NMR spectroscopy in the solid state: Very-fast sample rotation and multiple-quantum coherences, *Adv. Magn. Opt. Reson.,* submitted, (2001).

14. L. Müller, Sensitivity enhanced detection of weak nuclei using heternuclear multiple quantum coherence, *J. Am. Chem. Soc.* **101**, 4481–4484 (1979).

15. A. W. Hing, S. Vega, and J. Schaefer, Transferred-echo double-resonance NMR, *J. Magn. Reson.* **96**, 205–209 (1992).

16. A. W. Hing, S. Vega, and J. Schaefer, Measurement of heteronuclear dipolar coupling by transferred-echo double-resonance NMR, *J. Magn. Reson. A* **103**, 151–162 (1993).

17. C. A. Fyfe, K. T. Mueller, H. Grondey, and K. C. Wong-Moon,

18. E. R. H. van Eck and W. S. Veeman, Solid-state 2D-heteronuclear ^{27}Al–^{31}P correlation NMR spectroscopy of aluminophosphate VPI-5, *J. Am. Chem. Soc.* **115**, 1168–1169 (1993).

19. E. R. H. van Eck and W. S. Veeman, Spin density description of rotational-echo double-resonance, transferred-echo double-resonance and two-dimensional transferred-echo double-resonance solid state nuclear magnetic resonance, *Solid State Nucl. Magn. Reson.* **2**, 307–315 (1993).

20. C. A. Michal and L. W. Jelinski, REDOR 3D: Heteronuclear distance measurements in uniformly labeled and natural abundance solids, *J. Am. Chem. Soc.* **119**, 9059–9060 (1997).

21. K. Saalwächter and H. W. Spiess, Heteronuclear ^{1}H–^{13}C multiple-spin correlation in solid-state NMR: Combining REDOR recoupling and multiple-quantum spectroscopy, *J. Chem. Phys.,* submitted, (2001).

22. D. Sandström, M. Hong, and K. Schmidt-Rohr, Identification and mobility of deuterated residues in peptides and proteins by ^{2}H–^{13}C solid-state NMR, *Chem. Phys. Lett.* **300**, 213–220 (1999).

23. H. Geen, J. J. Titman, J. Gottwald, and H. W. Spiess, Spinning sidebands in the fast-MAS multiple-quantum spectra of protons in solids, *J. Magn. Reson. A* **114**, 264–267 (1995).

24. J. Gottwald, D. E. Demco, R. Graf, and H. W. Spiess, High-resolution double-quantum NMR spectroscopy of homonuclear spin pairs and proton connectivities in solids, *Chem. Phys. Lett.* **243**, 314–323 (1995).

25. U. Friedrich, I. Schnell, S. P. Brown, A. Lupulescu, D. E. Demco, and H. W. Spiess, Spinning-sideband patterns in multiple-quantum magic-angle spinning NMR spectroscopy, *Mol. Phys.* **95**, 1209–1227 (1998).

26. S. M. De Paul, unpublished results, 2000.

27. O. W. Sørensen, G. W. Eich, M. H. Levitt, G. Bodenhausen, and R. R. Ernst, Product operator formalism for the description of NMR pulse experiments, *Progr. NMR Spectrosc.* **16**, 163–192 (1983).

28. H. W. Spiess, Rotation of molecules and nuclear spin relaxation, *In* "NMR Basic Principles and Progress" (P. Diehl, E. Fluck, and R. Kosfeld, Eds.), Vol. 15, pp. 55–214, Springer-Verlag, Berlin (1978).

29. M. Mehring, "High Resolution NMR of Solids," Springer-Verlag, Berlin (1983).

30. K. Schmidt-Rohr and H. W. Spiess, "Multidimensional Solid-State NMR and Polymers," Academic Press, London (1994).

31. R. K. Hester, J. L. Ackerman, B. L. Neff, and J. W. Waugh, Separated local field spectra in NMR: Determination of structure of solids, *Phys. Rev. Lett.* **36**, 1081–1083 (1976).

32. J. E. Roberts, G. S. Harbison, M. G. Munowitz, J. Herzfeld, and R. G. Griffin, Measurement of heteronuclear bond distances in polycrystalline solids by solid-state NMR techniques, *J. Am. Chem. Soc.* **109**, 4163–4169 (1987).

33. G. A. Morris and R. Freeman, Enhancement of nuclear magnetic resonance signals by polarization transfer, *J. Am. Chem. Soc.* **101**, 760–761 (1979).

34. S. M. De Paul, K. Saalwächter, R. Graf, and H. W. Spiess, Sideband patterns from rotor-encoded longitudinal magnetization in MAS recoupling experiments, *J. Magn. Reson.* **146**, 140–156 (2000).

35. G. Bodenhausen and D. J. Ruben, Natural abundance nitrogen-15 NMR by enhanced heteronuclear spectroscopy, *Chem. Phys. Lett.* **69**, 185–189 (1980).

36. H. W. Spiess, Deuteron spin alignment: A probe for studying ultra-

slow motions in solids and solid polymers, *J. Chem. Phys.* **72,** 6755–6762 (1980).

37. M. M. Maricq and J. S. Waugh, NMR in rotating solids, *J. Chem. Phys.* **70,** 3300 (1979).

38. T. Gullion, D. B. Baker, and M. S. Conradi, New, compensated Carr–Purcell sequences, *J. Magn. Reson.* **89,** 479–484 (1990).

39. D. McElheny, E. DeVita, and L. Frydman, Heteronuclear local field NMR spectroscopy under fast magic-angle sample spinning conditions, *J. Magn. Reson.* **143,** 321–328 (2000).

40. J. M. Goetz and J. Schaefer, REDOR dephasing by multiple spins in the presence of molecular motion, *J. Magn. Reson.* **127,** 147–154 (1997).

41. K. Schmidt-Rohr, D. Nanz, L. Emsley, and A. Pines, NMR measurement of resolved heteronuclear dipole couplings in liquid crystals and lipids, *J. Phys. Chem.* **98,** 6668–6670 (1994).

42. C. Schmidt, K. J. Kuhn, and H. W. Spiess, Distribution of correlation times in glassy polymers from pulsed deuteron NMR, *Progr. Colloid Polymer Sci.* **71,** 71–76 (1985).

43. T. Terao, H. Miura, and A. Saika, Dipolar SASS NMR spectroscopy: Separation of heteronuclear dipolar powder patterns in rotating solids, *J. Chem. Phys.* **85,** 3816–3826 (1986).

44. J. L. Derissen, Crystal structure and conformation of methylmalonic acid, *Acta Crystallogr. B* **26,** 901 (1970).

45. M. S. Lehmann, T. F. Koetzle, and W. C. Hamilton, Precision neutron diffraction structure determination of protein and nucleic acid compounds. I. The crystal and molecular structure of the amino acid L-alanine, *J. Am. Chem. Soc.* **94,** 2657–2660 (1972).

46. K. Saalwächter and K. Schmidt-Rohr, Relaxation-induced dipolar exchange with recoupling—A novel MAS NMR method for determining heteronuclear distance without irradiating the second spin, *J. Magn. Reson.* **145,** 161–172 (2000).

47. C. A. Fyfe and A. R. Lewis, Investigation of the viability of solid-state NMR distance determinations in multiple spin systems of unknown structure, *J. Phys. Chem. B* **104,** 48–55 (2000).

48. T. Gullion and S. Vega, A simple magic angle spinning NMR experiment for the dephasing of rotational echoes of dipolar coupled homonuclear spin pairs, *Chem. Phys. Lett.* **194,** 423–428 (1992).

49. N. K. Sethi, Carbon-13 CP/MAS spectral assignment with one-dimensional separated-local-field spectroscopy, *J. Magn. Reson.* **94,** 352–361 (1991).

50. X. Wu and K. W. Zilm, Complete spectral editing in CPMAS NMR, *J. Magn. Reson. A* **102,** 205–213 (1993).

51. X. Wu, S. T. Burns, and K. W. Zilm, Spectral editing in CPMAS NMR. Generating subspectra based on proton multiplicities, *J. Magn. Reson. A* **111,** 29–36 (1994).

52. R. Sangill, N. Rastrup-Andersen, H. Bildsoe, H. J. Jacobsen, and N. C. Nielsen, Optimized spectral editing of ^{13}C MAS NMR spectra of rigid solids using cross polarization methods, *J. Magn. Reson. A* **107,** 67–78 (1994).

53. A. Lesage, S. Steuernagel, and L. Emsley, Carbon-13 spectral editing in solid-state NMR using heteronuclear scalar couplings, *J. Am. Chem. Soc.* **120,** 7095–7100 (1998).

54. S. T. Burns, X. Wu, and K. W. Zilm, Improvement of spectral editing in solids: A sequence for obtaining ^{13}CH + ^{13}CH$_2$-only ^{13}C spectra, *J. Magn. Reson.* **143,** 352–359 (2000).

55. J. Z. Hu, J. K. Harper, C. Taylor, R. J. Pugmire, and D. M. Grant, Modified spectral editing methods for ^{13}C CP/MAS experiments in solids, *J. Magn. Reson.* **142,** 326–330 (2000).

56. K. Schmidt-Rohr, J. Clauss, and H. W. Spiess, Correlation of structure, mobility, and morphological information in heterogeneous polymer materials by two-dimensional wideline-separation NMR spectroscopy, *Macromolecules* **25,** 3273–3277 (1992).

57. S. P. Brown, I. Schnell, J. D. Brand, K. Müllen, and H. W. Spiess, An investigation of π–π packing in a columnar hexabenzocoronene by fast magic-angle spinning and double-quantum ^{1}H solid-state NMR spectroscopy, *J. Am. Chem. Soc.* **121,** 6712–6718 (1999).

58. R. Graf, A. Heuer, and H. W. Spiess, Chain-order effects in polymer melts probed by ^{1}H double-quantum NMR spectroscopy, *Phys. Rev. Lett.* **80,** 5738–5741 (1998).

59. A. E. Bennett, C. M. Rienstra, M. Auger, K. V. Lakshmi, and R. G. Griffin, Heteronuclear decoupling in rotating solids, *J. Chem. Phys.* **103,** 6951–6958 (1995).